Loss of *O*-Linked Protein Glycosylation in *Burkholderia cenocepacia* Impairs Biofilm Formation and Siderophore Activity and Alters Transcriptional Regulators

Cameron C. Oppy,[a,b] Leila Jebeli,[a] Miku Kuba,[a] Clare V. Oates,[a] Richard Strugnell,[a] Laura E. Edgington-Mitchell,[b,c,d] Miguel A. Valvano,[e,f] Elizabeth L. Hartland,[a,g,h] Hayley J. Newton,[a] Nichollas E. Scott[a]

[a]Department of Microbiology and Immunology, University of Melbourne at the Peter Doherty Institute for Infection and Immunity, Melbourne, Australia
[b]Bio21 Molecular Science and Biotechnology Institute, University of Melbourne, Victoria, Australia
[c]Drug Discovery Biology, Monash Institute of Pharmaceutical Sciences, Monash University, Parkville, Victoria, Australia
[d]Department of Oral and Maxillofacial Surgery, New York University College of Dentistry, Bluestone Center for Clinical Research, New York, New York, USA
[e]Wellcome-Wolfson Institute for Experimental Medicine, Queen's University Belfast, Belfast, United Kingdom
[f]Department of Microbiology and Immunology, University of Western Ontario, London, Ontario, Canada
[g]Centre for Innate Immunity and Infectious Diseases, Hudson Institute of Medical Research, Clayton, Victoria, Australia
[h]Department of Molecular and Translational Science, Monash University, Clayton, Victoria, Australia

ABSTRACT *O*-linked protein glycosylation is a conserved feature of the *Burkholderia* genus. The addition of the trisaccharide β-Gal-(1,3)-α-GalNAc-(1,3)-β-GalNAc to membrane exported proteins in *Burkholderia cenocepacia* is required for bacterial fitness and resistance to environmental stress. However, the underlying causes of the defects observed in the absence of glycosylation are unclear. Using proteomics, luciferase reporter assays, and DNA cross-linking, we demonstrate the loss of glycosylation leads to changes in transcriptional regulation of multiple proteins, including the repression of the master quorum CepR/I. These proteomic and transcriptional alterations lead to the abolition of biofilm formation and defects in siderophore activity. Surprisingly, the abundance of most of the known glycosylated proteins did not significantly change in the glycosylation-defective mutants, except for BCAL1086 and BCAL2974, which were found in reduced amounts, suggesting they could be degraded. However, the loss of these two proteins was not responsible for driving the proteomic alterations, biofilm formation, or siderophore activity. Together, our results show that loss of glycosylation in *B. cenocepacia* results in a global cell reprogramming via alteration of the transcriptional regulatory systems, which cannot be explained by the abundance changes in known *B. cenocepacia* glycoproteins.

IMPORTANCE Protein glycosylation is increasingly recognized as a common posttranslational protein modification in bacterial species. Despite this commonality, our understanding of the role of most glycosylation systems in bacterial physiology and pathogenesis is incomplete. In this work, we investigated the effect of the disruption of *O*-linked glycosylation in the opportunistic pathogen *Burkholderia cenocepacia* using a combination of proteomic, molecular, and phenotypic assays. We find that in contrast to recent findings on the *N*-linked glycosylation systems of *Campylobacter jejuni*, *O*-linked glycosylation does not appear to play a role in proteome stabilization of most glycoproteins. Our results reveal that loss of glycosylation in *B. cenocepacia* strains leads to global proteome and transcriptional changes, including the repression of the quorum-sensing regulator *cepR* (*BCAM1868*) gene. These alterations lead to dramatic phenotypic changes in glycosylation-null strains, which are paralleled by both global proteomic and transcriptional alterations, which do not appear to directly result from the loss of glycosylation per se. This research unravels the pleiotropic effects of *O*-linked glycosylation in *B. cenocepacia*, demonstrating that its loss

does not simply affect the stability of the glycoproteome, but also interferes with transcription and the broader proteome.

The *Burkholderia cepacia* complex (Bcc) includes diverse and ubiquitous, phylogenetically related Gram-negative species (1). To date, 20 Bcc species have been identified (1–3), but the commonality of Bcc in the environment (2, 3) and their recognition as opportunistic pathogens (4–6) continually drives the identification of new Bcc members. Within clinical settings, Bcc can lead to fatal infections (7, 8) that are challenging to control with antibiotic therapies (9) and can be spread by patient-to-patient transmission (10, 11). This is especially problematic for Bcc infections in people with cystic fibrosis (CF), where Bcc infections result in accelerated loss of lung function (12) as well as increased morbidity and mortality compared to other infectious agents (13, 14). *B. cenocepacia* is one of the most common Bcc species isolated from CF patients across the globe (15–18) and is generally associated with more fulminant disease leading to higher mortality than observed with other Bcc species (19). One of the most serious clinical outcomes from *B. cenocepacia* infections in people with CF is a condition known as "cepacia syndrome," an unrelenting necrotizing pneumonia that rapidly leads to respiratory failure, bacteremia, and death (20). Although interventions with antimicrobial therapies can stop or even reverse cepacia syndrome (20), the intrinsic resistance of Bcc to multiple classes of antibiotic (21–23) and their propensity to form biofilms (24) make treatment success variable at best (9). To improve clinical outcomes, it is therefore essential to better understand the factors contributing to the ability of *B. cenocepacia* to infect immunocompromised hosts.

Biofilm formation is associated with bacterial persistence and the failure of antimicrobial treatments in a range of pathogens (25). Bcc members, including *B. cenocepacia*, produce biofilms on abiotic (26, 27) and biotic (28) surfaces. However, *B. cenocepacia* bacteria in the CF lung do not appear to form true biofilms, but instead are observed extracellularly as small clusters surrounded by mucus and mainly within phagocytic cells in the submucosal tissue (29, 30). Increased biofilm production is associated with bacterial persistence in CF patients (31), and mutations selected for during chronic infections in CF patients mirror those observed during biofilm *in vitro* evolution experiments (32). The ability to form biofilms in Bcc, as well as the expression of multiple virulence factors, is controlled by numerous quorum sensing (QS) systems (33). A key class of QS systems associated with Bcc virulence are based on homoserine lactones (HSLs) (24). Across the Bcc, some HSL QS systems are variable or lineage specific, such as CciR/I and CepR2 (34, 35), while others are highly conserved in all members. One such highly conserved HSL QS system is the CepR/I regulon (36, 37), which generates *N*-octanoylhomoserine lactone (C$_8$-HSL) using the HSL synthase CepI (BCAM1870), which in turns activates the transcriptional regulator CepR (37, 38). CepR (BCAM1868) is a major regulator of biofilm formation (39), and disruption of CepR/I attenuates Bcc virulence in several models (40, 41) and reduces disease severity (40, 42). The importance of the CepR/I QS system in Bcc virulence stems from its broad regulatory profile affecting multiple virulence-associated genes (43–45), such as those encoding the secreted zinc metalloproteases ZmpA (46) and ZmpB (47), siderophore production (39, 48), and the key mediator of biofilm formation protein A (BapA) (45).

Glycosylation is increasingly recognized as a common posttranslational modification in bacterial systems (49–56). Many glycosylation systems are conserved across bacterial genera (57, 58) and phyla (59, 60), suggesting glycosylation is critical for optimal proteome functionality. Disruption of glycosylation pathways in several species results in reduced fitness compared to glycosylation-competent strains (52–56). However, the underlying cause of fitness reduction remains poorly defined (61, 62). Only recently have mechanistic insights emerged on how the loss of glycosylation affects bacterial physiology and pathogenesis. In *Campylobacter jejuni*, loss of glycosylation results in

decreased stability of the majority of known glycoproteins, which in turn affects virulence (63, 64). These data support a model whereby bacterial *N*-linked glycosylation contributes to protein stability, but it is unclear whether other glycosylation systems, such as *O*-linked glycosylation, have evolved to stabilize glycosylated proteins.

Previously, we reported *B. cenocepacia* possesses an *O*-linked glycosylation system responsible for the modification of at least 23 proteins with a trisaccharide glycan using the enzyme PglL (BCAL0960) (56). Building on this work, we recently identified the biosynthetic locus, the <u>O</u>-glycosylation <u>c</u>luster (OGC [BCAL3114 to BCAL3118]), responsible for the generation of the *O*-linked glycan, established the *O*-linked glycan structure as β-Gal-(1,3)-α-GalNAc-(1,3)-β-GalNAc, and demonstrated that glycosylation was required for optimal bacterial fitness and resistance to clearance in the *Galleria mellonella* infection models (65). Although these studies have demonstrated a link between glycosylation and bacterial fitness, the mechanism remains unclear. Using quantitative proteomic approaches, we sought to understand the proteome changes resulting from the loss of *O*-linked glycosylation in *B. cenocepacia*. We demonstrated that loss of glycosylation in *B. cenocepacia* resulted in global proteome alterations beyond the known glycoproteome, which are associated with widespread alterations in transcriptional regulation. We discovered that the HSL QS system CepR/I is repressed in glycosylation-defective mutants, and this coincides with defective biofilm formation and reduced siderophore activity. In contrast to the loss of glycosylation in *C. jejuni*, we also demonstrate that only a few glycoproteins are reduced in abundance in the absence of glycosylation, but they are not responsible for the glycosylation-null phenotypes. Together, our data indicate that the roles of glycosylation in *B. cenocepacia* extend beyond protein stabilization, and loss of *O*-linked glycosylation in *B. cenocepacia* causes dramatic physiological changes due to alterations in transcriptional regulatory systems and the proteome at large.

RESULTS

Loss of glycosylation in *B. cenocepacia* leads to global proteome alterations.
We previously demonstrated that loss of glycosylation causes defects in motility (56), reduction of virulence in plant and insect infection models (56, 65), and defects in carbon utilization (65). To better understand the role of glycosylation in *B. cenocepacia*, we assessed the effect of loss of glycosylation on the proteome. To achieve this, we generated markerless deletion mutations in the *O*-oligosaccharyltransferase *pglL* gene ($\Delta pglL$ [BCAL0960]) (56), the recently identified *O*-linked glycan cluster (ΔOGC [BCAL3114 to BCAL3118]) responsible for the generation of the glycan used for *O*-linked glycosylation (65), and a double-glycosylation-null strain ($\Delta pglL$ ΔOGC). We also constructed a chromosomal *pglL* complemented strain ($\Delta pglL$ *amrAB*::S7-*pglL*-His$_{10}$) (see Fig. S1A in the supplemental material). The rationale for creating multiple glycosylation-defective strains was to eliminate potential confounding effects arising from blocking glycosylation at a specific step and the corresponding accumulation of unprocessed lipid-linked glycans. Western blot analysis using the glycoprotein acceptor protein DsbA$_{Nm}$-His$_6$ (56, 66) supported the loss of glycosylation in the $\Delta pglL$, ΔOGC, and $\Delta pglL$ ΔOGC strains, as well as restoration of glycosylation in the $\Delta pglL$ *amrAB*::S7-*pglL*-His$_{10}$ strain (Fig. 1A). In contrast to our previously reported plasmid-based PglL complementation approaches (56) chromosomal complementation lead to the restoration of glycosylation to near wild-type (WT) levels (Fig. S1B) as well as restoration of motility (Fig. S1C) compared to only partial restoration previously reported (56).

Using label-free quantification (LFQ)-based quantitative proteomics, 5 biological replicates of each strain were investigated, leading to the identification of 3,399 proteins with 2,759 proteins quantified in at least 3 biological replicates in a single biological group (see Fig. S2A and B and Data Set S1, tab 1, in the supplemental material). As expected, no glycopeptides were observed in the $\Delta pglL$, $\Delta pglL$ ΔOGC, and ΔOGC strains, while multiple glycopeptides were observed in the wild-type and $\Delta pglL$ *amrAB*::S7-*pglL*-His$_{10}$ strains (Fig. S1D). Hierarchical clustering of Pearson correlations of proteome samples demonstrated robust correlation between all samples (average
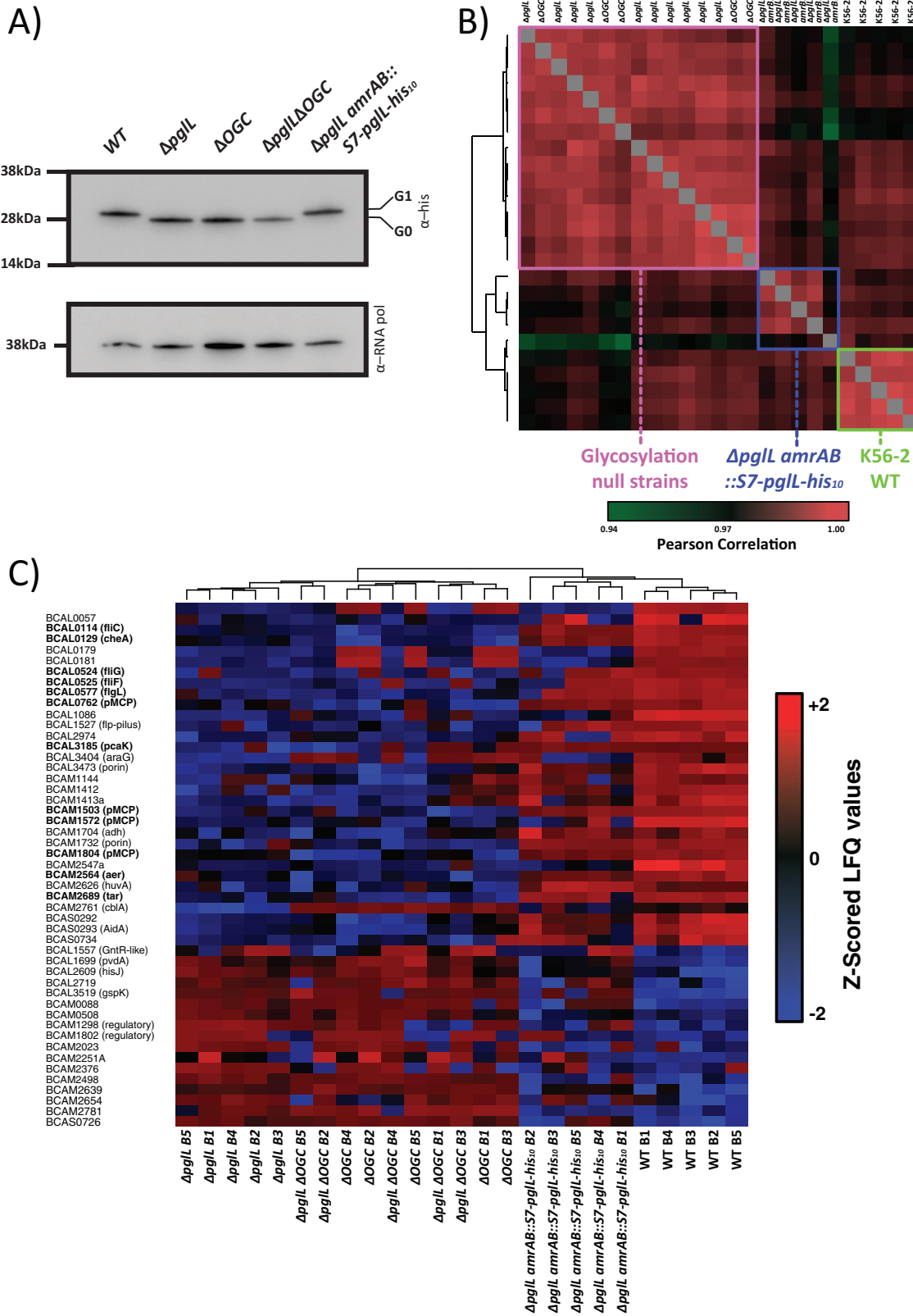
FIG 1 Disruption of O-linked glycosylation results in multiple changes in the proteome. (A) Western analysis of strains expressing the glycosylation substrate DsbA$_{Nm}$-His$_6$ confirms the loss of glycosylation in the Δ*pglL*, ΔOGC, and Δ*pglL* ΔOGC mutant strains and
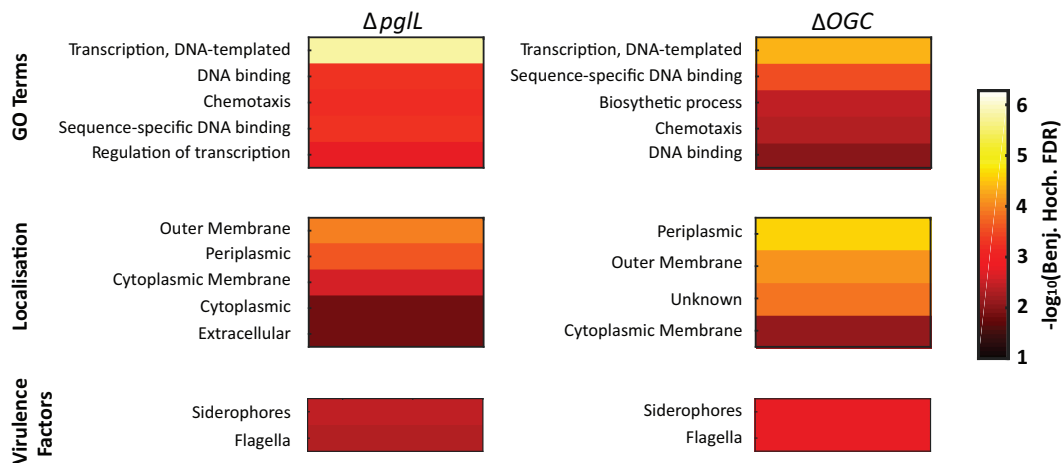
(Continued on next page)

FIG 2 Heat maps of glycosylation-null strain enrichment analysis. The multiple hypothesis corrected *P* values from Fisher's exact tests demonstrate that proteins with similar GO terms and localizations and associated with virulence factors are altered in glycosylation-null strains.

Pearson correlation of 0.98 [Data Set S1, tab 2]); yet three discrete proteome clusters were readily identified separating the wild-type K56-2 and Δ*pglL amrAB*::S7-*pglL*-His$_{10}$ strains and the glycosylation-null strains (Fig. 1B). Examination of the most profound alterations, proteins with a −log$_{10}$ *P* value of >3 and a fold change greater than ±2 log$_2$ units, revealed alterations in protein levels observed in the Δ*pglL* mutant that were mirrored in the ΔOGC and Δ*pglL* ΔOGC strains, which were restored by complementation (Fig. 1C). Consistent with the observed motility defects (Fig. S1C), the levels of proteins associated with flagellum-mediated motility and chemotaxis, including BCAL0114 (FliC), BCAL0129 (CheA), BCAL0524 (FliG), and BCAL0525 (FliF), were significantly reduced in glycosylation-null strains. Importantly, multiple known virulence-associated proteins were also decreased in the glycosylation-null strains, including the heme receptor protein HuvA (BCAM2626 [67]) and nematocidal protein AidA (BCAS0293 [68]). Numeration of the overlap of all altered protein between glycosylation-null strains by Fisher exact enrichment analysis demonstrated a substantial enrichment between these three groups (Fisher's exact test, 6.7502 × 10^{177} and 4.3784 × 10^{245} for the Δ*pglL* compared with ΔOGC strain, and for the Δ*pglL* compared with Δ*pglL* ΔOGC strain, respectively) (Data Set S1, tab 3, and Fig. S2C). These results revealed that the loss of glycosylation due to disruption of *pglL* or OGC leads to similar changes, which are largely complemented to parental levels by reintroduction of *pglL* in the chromosome.

Loss of glycosylation results in reduction in CepR/I transcription and the levels of DNA-associated CepR. Enrichment analysis of the altered proteins in glycosylation-null strains demonstrate the over representation of a range of categorical groups based on GO (Gene Ontology) terms, protein localization, and virulence-associated factor assignments. These groups highlight that protein localization assignments and virulence-associated factors were similarly affected in Δ*pglL* and ΔOGC strains, recapitulating observations made at the individual protein level (Fig. 2; Data Set S1, tab 3). Interestingly, enrichment analysis highlighted the link between the loss of *O*-linked glycosylation and changes that were broader than only motility and virulence. For example, differences also observed in proteins associated with DNA-sequence specific

FIG 1 Legend (Continued)
restoration of glycosylation in the Δ*pglL amrAB*::S7-*pglL*-His$_{10}$ chromosomal complemented strain. (B) Pearson correlation analysis demonstrates three discrete clusters observed across the proteomic analysis which separate glycosylation-competent and glycosylation-null strains. (C) Z-scored heat map of proteins observed to undergo alterations between glycosylation-competent and glycosylation-null strains reveals alterations in motility and chemotaxis (proteins in boldface), including BCAL0114 (FliC), BCAL0524 (FliG), and BCAL0525 (FliF), as well as known CepR-regulated protein BCAS0293 (AidA).

binding and transcriptional regulation (Fig. 2; Data Set S1, tab 3). This observation suggested that loss of glycosylation results in alterations in the transcriptional landscape of *B. cenocepacia*. As virulence is coordinated by global regulators such as CciR, CepR, ShvR, and AtsR in *B. cenocepacia* (35, 43, 69, 70), we assessed if known regulators could account for the observed proteome changes in glycosylation-null strains. As our data demonstrated minimal alteration of the regulator ShvR (BCAS0225; Data Set S1, tab 1) across the analyzed strains, and disruption of both *atsR* (BCAM0379) and *cciR* (BCAM0240) has previously been associated with increased motility (43, 69), we reasoned that the regulator CepR (BCAM1868) may be responsible for the glycosylation-dependent differences in our mutant strains. Although CepR is observed within our proteomic analysis, its low intensity prevented accurate quantitation across all strains (Data Set S1, tab 1). However, the stringently CepR-regulated AidA protein (BCAS0293 [45, 71]) exhibited decreases of -2.9 and -3.1 $\log_2$ within $\Delta pglL$ and ΔOGC strains compared to the WT (Fig. 1C), indicating reduced CepR levels. This observation prompted us to investigate regulation of other known CepR-regulated genes and proteins. Using available microarray data of CepR-regulated genes (43), we investigated the correlation of the proteome changes observed in the absence of glycosylation, with alterations observed in response to the disruption of CepR. We observed a statistically significant enrichment of CepR-regulated proteins altered in the absence of glycosylation (multiple hypothesis corrected P values of 1.79×10^6 and 6.69×10^6 for the $\Delta pglL$ and ΔOGC strains, respectively [Data Set S1, tab 3]), supporting a link between CepR and the alteration observed in glycosylation-null strains and suggesting that the loss of glycosylation may influence the *B. cenocepacia* CepR regulon.

To determine transcriptional changes in *cepR/I* genes, we introduced the *cepR* and *cepI* luciferase promoter reporter (pPromcepR [69] and pCP300 [72]) into the wild-type K56-2, mutant $\Delta pglL$, and complemented $\Delta pglL$ *amrAB*::S7-*pglL*-His$_{10}$ strains. As expected from the proteomic results, the $\Delta pglL$ strain showed decreased induction of both *cepI* and *cepR* over a 24-h period (Fig. 3A; see Fig. S3 in the supplemental material) compared with the wild-type and $\Delta pglL$ *amrAB*::S7-*pglL*-His$_{10}$ strains. Detailed examination at 12 h (log phase), 16 h (the transition from log to stationary phase), and 20 h (stationary phase) revealed higher levels of transcription in the wild type of both *cepI* and *cepR* at 16 and 20 h compared with transcription levels in the $\Delta pglL$ mutant, despite comparable growth kinetics (see Fig. S4A and B in the supplemental material). As the C$_8$-HSL levels affect the response of CepI and CepR in *B. cenocepacia* (39, 44, 73), we assayed *cepR/I* transcription in the absence and presence of additional C$_8$-HSL (10 μM [Fig. 3B]). In response to exogenous C$_8$-HSL, *cepI* transcription increased in all strains (Fig. 3B), consistent with the positive-feedback response expected to heighten C$_8$-HSL levels (39, 44). In contrast, while the addition of C$_8$-HSL led to no change in *cepR* transcription in the $\Delta pglL$ mutant, it resulted in reduced transcription of *cepR* to the level observed in the wild-type K56-2 strain. Complementation of *pglL*, using *amrAB*::S7-*pglL*-His$_{10}$, restored CepI transcription to wild-type levels but only partially restored CepR transcription (Fig. 3B). As expected from the reduction in *cepR/I* transcription resulting from the loss of glycosylation, *cepR* and *cepI* transcription was also compromised in ΔOGC strains (Fig. S4C to F). Together, these results indicate that both *cepR* and *cepI* transcription are altered in the loss of glycosylation, with the resulting *cepR* levels resembling the levels observed during C$_8$-HSL-induced repression in wild type.

As the CepR protein autoregulates *cepR*'s own transcription (48), we reasoned that the decreased transcription in the $\Delta pglL$ mutant would correspond to decreased levels of DNA-bound CepR. To directly assay DNA binding by CepR, we monitored the DNA-bound proteome using formaldehyde-based cross-linking coupled to DNA enrichment (74). Initial analysis of the DNA-bound proteome found glycosylation-null strains ($\Delta pglL$ and ΔOGC) and glycosylation-proficient strains (wild type and $\Delta pglL$ *armAB*::S7-*pglL*-His$_{10}$) possessed distinct proteome profiles with multiple uncharacterized transcriptional regulators (e.g., BCAL0946, BCAL1916, BCAS0168, BCAL2309, and BCAL0472) which were altered by the loss of glycosylation (Fig. 3C; Data Set S1, tab 4). Although this analysis enabled the identification of CepR, its low abundance prevented its
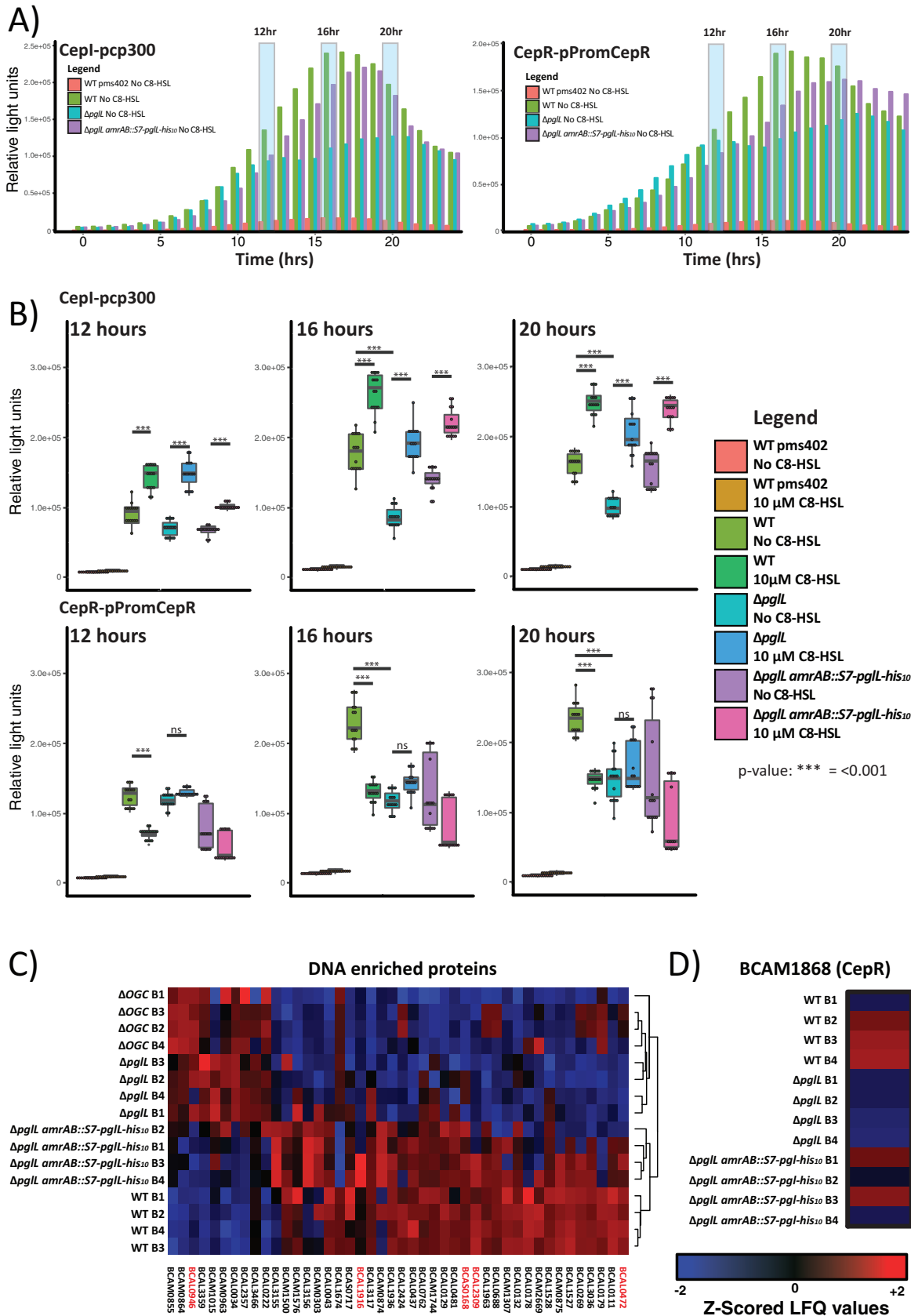
FIG 3 CepR/I transcription is altered in glycosylation-null strains. (A) Twenty-four-hour luciferase profile of strains grown with either the CepI reporter pCP300 or CepR reporter pPromCepR demonstrating alteration in luciferase activity in the Δ*pglL* mutant compared to the
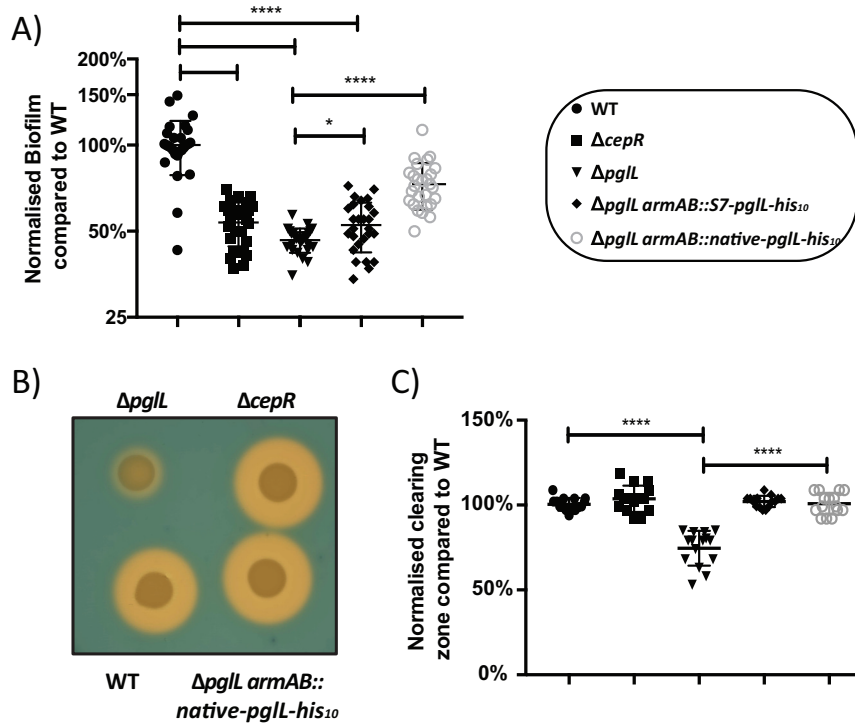
(Continued on next page)

FIG 4 Biofilm formation and siderophore activities are reduced in the ΔpglL mutant. (A) Twenty-four-hour static biofilm assays demonstrate a decrease in biofilm formation in the ΔpglL strain, which is partially restored upon complementation. (B and C) CAS assays demonstrate a reduction in the zone of clearing in the ΔpglL mutant, which is restored upon complementation.

quantitation across biological replicates. To improve the monitoring of CepR, targeted proteomic analysis was undertaken using PRM assays, which confirmed the reduction in DNA-associated CepR in the ΔpglL mutant compared with the wild-type and ΔpglL armAB::S7-pglL-His$_{10}$ strains (Fig. 3D [$P = 0.017$ for wild type versus ΔpglL strain]; Data Set S1, tab 5). In agreement with the total proteome and lux reporter measurements, the DNA-bound proteome supports multiple transcription-associated proteins, including the global regulator CepR, that are altered in the absence of glycosylation.

The ΔpglL mutant demonstrates a reduced ability to form biofilms and produce siderophores. The observed reductions in CepR/I transcription suggested that CepR/I-linked phenotypes may also be altered in glycosylation-null strains. To test this hypothesis, we assessed two phenotypes associated with CepR/I regulation: (i) the production of biofilm under static 24-h growth and (ii) siderophore activity (39, 43–45, 48). Consistent with an impact of glycosylation on known CepR/I-regulated phenotypes, we observed a marked reduction in biofilm formation in the ΔpglL mutant, which was partially restored by complementation (Fig. 4A). Interestingly, we also observed that the method of complementation—i.e., expression of PglL-His$_{10}$ driven from the native pglL promoter (ΔpglL amrAB::native-pglL-His$_{10}$) or from the constitutive S7 promoter (ΔpglL amrAB::S7-pglL-His$_{10}$)—affected the restoration of biofilm formation

FIG 3 Legend (Continued)

WT and ΔpglL amrAB::S7-pglL-His$_{10}$ complemented strains. Each data point corresponds to the mean of three independent biological replicates with a more detailed figure containing the plotted standard deviation provided in Fig. S3. (B) Detailed analysis of three time points across the luciferase profiles are provided for the 12-h (log phase), 16-h (transition from log to stationary phase), and 20-h (stationary phase) time points. For each time point, the luciferase activities of strains grown with and without C$_8$-HSL are shown. (C) Z-scored heat map of DNA-bound proteins with significant alterations in abundance in the ΔpglL or ΔOGC mutant compared to the WT reveal similar protein profiles for glycosylation-null strains compared to glycosylation-competent strains. (D) DNA bound proteome analysis of CepR supports the reduction in the abundance of DNA-bound CepR in the ΔpglL strain and the partial restoration of CepR in the ΔpglL amrAB::S7-pglL-His$_{10}$ strain.

(Fig. 4A). Examination of independently created Δ*pglL* and Δ*pglL amrAB*::native-*pglL*-His$_{10}$ strains confirmed a link between biofilm formation through phenotype restoration by complementation (see Fig. S5A in the supplemental material). Chrome azurol S (CAS) assays, used to assess the global levels of siderophore activity, demonstrated a reproducible effect in the Δ*pglL* mutant, which was completely restored by complementation when PglL was expressed from either its native or the S7 promoter (Fig. 4B and C). The ΔOGC and ΔOGC Δ*pglL* strains also demonstrate biofilm and siderophore alterations compared to the wild type, although these alterations were not completely identical to those observed in the Δ*pglL* mutant (Fig. S5B to D). Together, we conclude that phenotypes associated with CepR/I regulation, including biofilm and siderophore activity, are affected by the loss of glycosylation.

Except for BCAL1086 and BCAL2974, proteins that are normally glycosylated remain stable in the absence of glycosylation. As the loss of glycosylation in other bacterial glycosylation systems leads to protein instability (63, 64, 75), we examined whether protein instability in *B. cenocepacia* may be responsible for the phenotypic changes in glycosylation-null strains. Our proteomic analysis identified 21 out of 23 known glycoproteins (56), yet only 2 were altered in abundance in glycosylation-negative strains: BCAL1086 (−5.7 log$_2$) and BCAL2974 (−2.5 log$_2$) (Fig. 5A; Data Set S1, tab 1). To confirm the observed decreases in abundance, endogenous BCAL1086 and BCAL2974 were His$_{10}$ tagged at the C terminus. While His tagging did not allow the detection of BCAL2974 by Western analysis (data not shown), the introduction of the His$_{10}$ epitope into BCAL1086 allowed quantification of endogenous BCAL1086 in the K56-2 wild-type, Δ*pglL* mutant, and Δ*pglL amrAB*::S7-*pglL*-His$_{10}$ complemented strain backgrounds and confirmed the loss of BCAL1086 in the Δ*pglL* mutant (Fig. 5B). We sought to directly assess whether BCAL1086 was subjected to increased degradation in the Δ*pglL* mutant, as a measure of instability. For this, we monitored the endogenous peptide pool (76), quantifying peptides derived from 783 proteins (Data Set S1, tabs 6 and 7) in the *B. cenocepacia* K56-2 wild-type, Δ*pglL* mutant, and Δ*pglL amrAB*::S7-*pglL*-His$_{10}$ complemented strain. Consistent with the degradation of BCAL1086, we observed an increase in the abundance of BCAL1086-derived peptides in the Δ*pglL* mutant, while peptides from other known glycoproteins showed only modest changes (Fig. 5C; Data Set S1, tab 7). Within this peptidomic analysis, we observed that multiple unique BCAL1086 peptides were present in the Δ*pglL* mutant clustered around the central region of BCAL1086 (Fig. 5D), confirming that BCAL1086 was expressed in the Δ*pglL* mutant, but subjected to proteolysis. Together, our data support that BCAL1086 becomes degraded in the absence of glycosylation, but the majority of known *B. cenocepacia* glycoproteins are unaffected.

Role of BCAL1086 and BCAL2974 in Δ*pglL* phenotypes. As changes in the glycoproteins BCAL2974 and BCAL1086 coincided with an alteration in biofilm and siderophore activity, we investigated if the loss of BCAL2974 and BCAL1086 could be responsible for defects observed in the Δ*pglL* mutant. To answer this question, Δ*BCAL2974* and Δ*BCAL1086* strains were created and assessed for their effect on biofilm production and siderophore activity, as well as virulence in *G. mellonella*, a phenotype previously associated with Δ*pglL* mutation (56). Both BCAL1086 and BCAL2974 have no known functions and lack homology to known domains but are present in multiple *Burkholderia* species. Assessment of 24-h static biofilm growth showed the Δ*BCAL1086* mutation had no effect on biofilm formation, while Δ*BCAL2974* resulted in a small but reproducible decrease in biofilm development. However, this effect is minimal compared to the defect observed in Δ*pglL* and Δ*cepI* mutants (Fig. 6A). The ability of Δ*BCAL1086* and Δ*BCAL2974* mutants to produce siderophores was unaffected (Fig. 6B and C). Similarly, while *G. mellonella* infections showed that Δ*pglL* causes reduced mortality at 48 h postinfection compared to in the K56-2 WT (*P* = 0.0015), Δ*BCAL2974*, Δ*BCAL1086*, and Δ*pglL amrAB*::native-*pglL*-His$_{10}$ strains demonstrated wild-type levels of lethality in *G. mellonella* at 48 h (Fig. 6D). These results suggest that even though
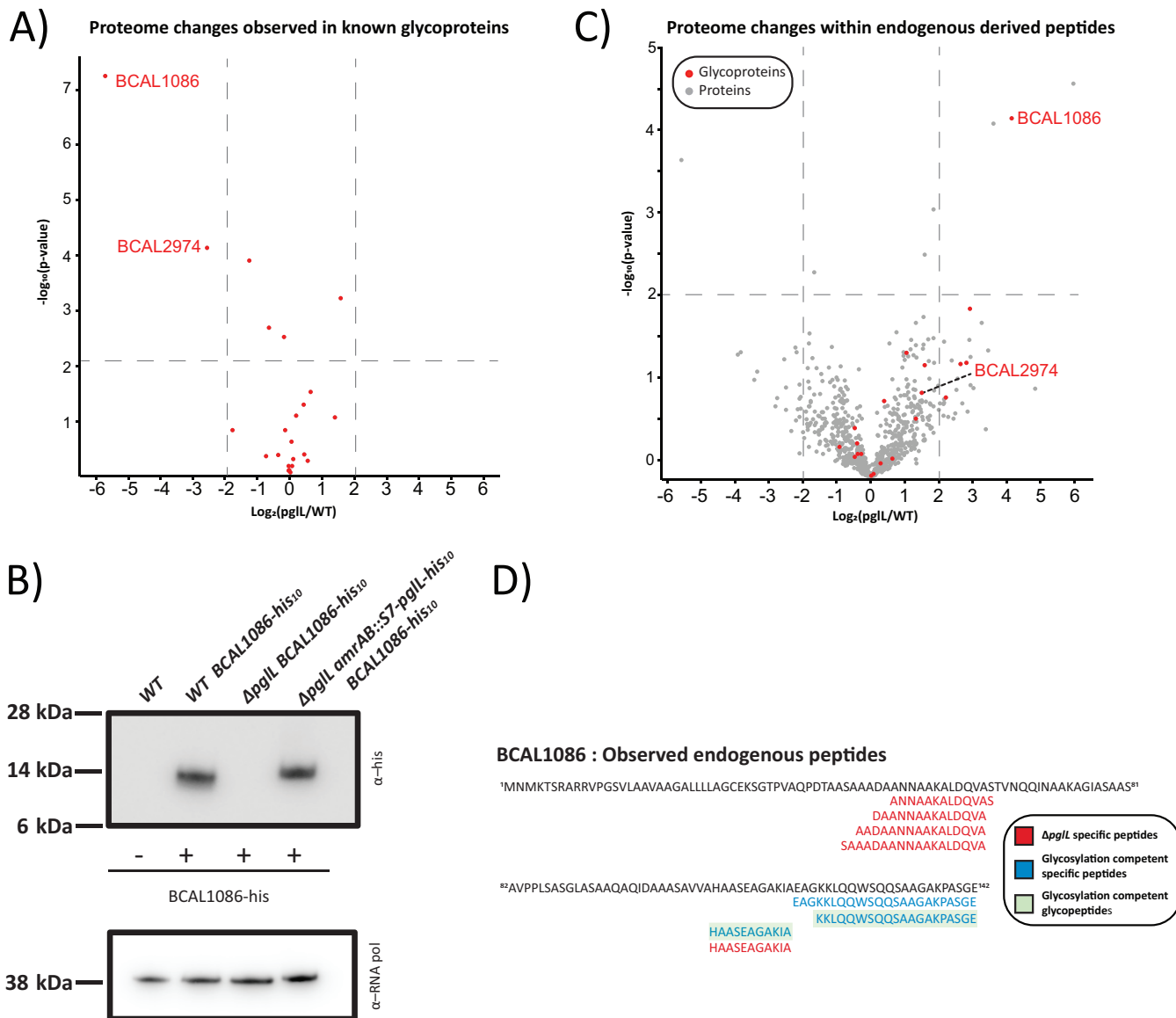
FIG 5 The stability of glycoproteins BCAL1086 and BCAL2974 is affected by loss of glycosylation. (A) Proteomic analysis demonstrates BCAL1086 and BCAL2974 decrease in abundance in the absence of glycosylation. (B) Endogenous tagging of BCAL1086 confirms the loss of BCAL1086 in the ΔpglL background. (C) Proteomic analysis of endogenous derived peptides demonstrates an increased abundance of BCAL1086-derived peptides in the absence of glycosylation. (D) Analysis of endogenous peptides confirms the presence of unique peptide fragments from BCAL1086 in the ΔpglL background.

BCAL2974 and BCAL1086 are influenced by the loss of glycosylation, neither protein is solely responsible for the known defect observed in the ΔpglL mutant.

We also investigated whether the loss of either BCAL2974 or BCAL1086 drives proteome changes. Using label-free-based quantitative proteomics, we compared the proteomes of the K56-2 WT, ΔBCAL2974, ΔBCAL1086, ΔpglL, ΔcepR, Δcepl, and ΔpglL amrAB::S7-pglL-His$_{10}$ to assess the similarity between the proteomes as well as the specific proteins affected by the loss of these proteins. Proteomic analysis led to the identification of 3,730 proteins, with 2,752 proteins quantified in at least 3 biological replicates in a single biological group (Data Set S1, tab 8). Clustering of the proteomic analysis revealed that ΔBCAL2974 and ΔBCAL1086 strains closely grouped with the WT strains, while the ΔpglL, ΔcepR, Δcepl, and ΔpglL amrAB::S7-pglL-His$_{10}$ strains formed discrete clusters. This macroanalysis indicated that mutations in BCAL2974 or BCAL1086 had a minimal effect on the proteome (Fig. 7A; Data Set S1, tabs 9 and 10). Supporting this conclusion, analysis of the specific proteins that varied between the different
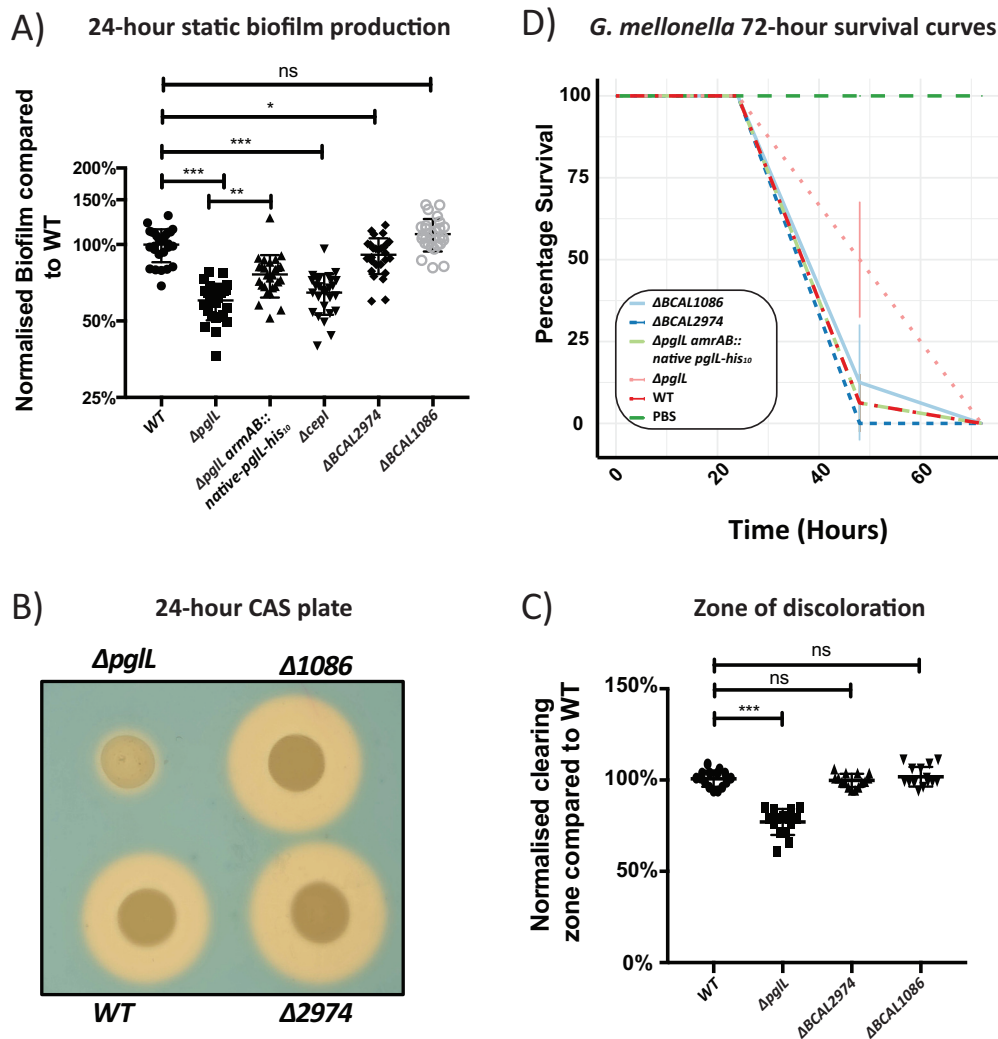
FIG 6 The loss of BCAL1086 or BCAL2974 does not affect phenotypes associated with Δ*pglL* mutation. (A) Twenty-four-hour static biofilm formation is unaffected in the Δ*BCAL1086* mutant and minimally affected in the Δ*BCAL2974* mutant compared to the WT. (B) CAS plate assays demonstrate similar zones of clearing in the Δ*BCAL1086* and Δ*BCAL2974* strains compared to the K56-2 parent strain. (C) Quantification of the zone of clearing demonstrates no significant alteration in siderophore activity in Δ*BCAL1086* and Δ*BCAL2974* mutants compared to the K56-2 parent strain. (D) Survival curve of *G. mellonella* infections. Data from three independent replicates of 8 to 10 larvae for each biological group are shown with the standard deviation also denoted. The Δ*BCAL1086* and Δ*BCAL2974* strains mirror the lethality of the WT and Δ*pglL amrAB*::native-*pglL*-His$_{10}$ strains.

strains demonstrated few proteome alterations in the Δ*BCAL2974* and Δ*BCAL1086* mutants compared with the Δ*pglL*, Δ*cepR*, and Δ*cepI* mutants (Fig. 7B), with the Δ*cepR*, Δ*cepI*, and Δ*pglL* strains also demonstrating the expected similarity in their proteome changes (Fisher exact test, Δ*cepR* versus Δ*pglL* strain, $P = 3.25 \times 10^5$, and Δ*cepI* versus Δ*pglL* strain, $P = 6.95 \times 10^4$ [Data Set S1, tab 11]). Taken together, the proteome analysis results support the contention that BCAL2974 and BCAL1086 have minimal effects on the proteome and are not responsible for the broad proteomic alterations observed in the Δ*pglL* mutant.

DISCUSSION

Although glycosylation is a common protein modification in bacterial species (49–51, 77) our understanding of how this modification influences bacterial physiology and pathogenesis is unclear. Recent insights into how glycosylation impacts bacterial proteomes have been obtained through study of the archetypical *N*-linked glycosylation system of *C. jejuni* (78, 79), yet it is unclear whether these observations are
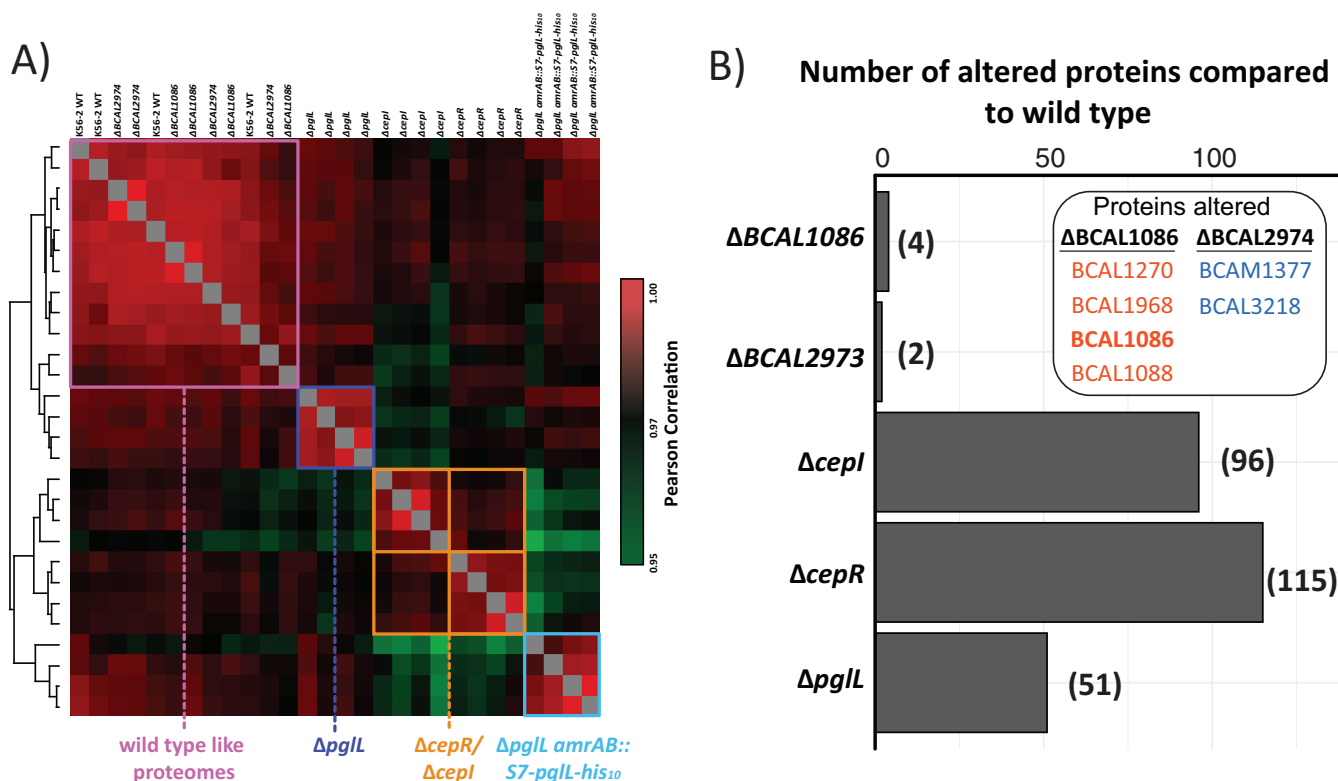
FIG 7 Disruption of *BCAL1086* and *BCAL2974* does affect the proteome like the Δ*pglL* mutation. (A) Pearson correlation analysis of the K56-2 WT, Δ*BCAL2974*, Δ*BCAL1086*, Δ*pglL*, Δ*cepR*, Δ*cepI*, and Δ*pglL amrAB*::S7-*pglL*-His$_{10}$ proteomes demonstrates K56-2 WT, Δ*BCAL2974*, and Δ*BCAL1086* biological replicates cluster together, while other strains form discrete clusters. (B) Quantitative proteome analysis of Δ*BCAL1086*, Δ*BCAL2974*, Δ*cepI*, Δ*cepR*, and Δ*pglL* mutants compared to the wild type demonstrates minor proteome alterations compared to the Δ*cepI*, Δ*cepR*, and Δ*pglL* mutants.

generalizable to other glycosylation systems such as *O*-linked glycosylation systems. Studies on the role of *N*-linked glycosylation within *C. jejuni* have revealed that defects associated with the loss of glycosylation stem from the loss of glycoproteins (78, 79), suggesting that *N*-linked glycosylation extends protein longevity in *C. jejuni*. In contrast, we find here that loss of *O*-linked glycosylation in *B. cenocepacia* has a more limited effect on the proteins targeted for glycosylation with only a subset of the known glycoproteins being affected by the disruption of glycosylation (Fig. 5). Therefore, the defect associated with loss of O-linked glycosylation in *B. cenocepacia* cannot be merely explained by protein instability. Indeed, we demonstrate that loss of glycosylation leads to changes in the expression of nonglycosylated proteins whose expression is regulated by the CepR/I regulon (Fig. 3) (39, 42, 48). Therefore, our findings uncover a previously unknown link between loss of glycosylation and alterations in pathways controlled by global transcriptional regulators.

The observation that biofilm formation is reduced in the Δ*pglL* mutant mirrors previous reports in *Acinetobacter baumannii* (55) and *C. jejuni* (63), but the link of this phenotype to alterations in regulations has not previously documented. Previous studies in *B. cenocepacia* have identified that not all CepR/I-regulated proteins are required for biofilm formation. However, BapA (BCAM2143) plays a major role in the formation of biofilms on abiotic surfaces, whereas the lectin complex BclACB (BCAM0184 to BCAM0186) contributes to biofilm structural development (45). Although BapA (BCAM2143) was not detected in any of our proteomic analyses, BclA and BclB (BCAM0186 and BCAM0184, respectively) were decreased in the Δ*pglL* mutant (both with a −1.0-log$_2$ decrease compared with the WT; −log$_{10}$ *P* > 3.05 [Data Set S1, tab 1]). Surprisingly, BclA and BclB increased in abundance in Δ*pglL* ΔOGC and ΔOGC strains (both 1.0 log$_2$ increases compared with WT; −log$_{10}$ *P* > 1.4 [Data Set S1, tab 1]),

and these mutants formed extensive biofilms (Fig. S5B). This result agrees with recent work showing that with disruption of *BCAL3116*, the third gene in the OGC, resulted in enhanced biofilm formation (80). It also should be noted that within this study, we observed that the method of complementation of *pglL* also influenced the restoration of biofilm formation (Fig. 4A). As differences between the promoter used to drive *pglL* expression can influence some glycosylation-null phenotypes, this supports the hypothesis that *pglL* itself may be regulated under specific conditions. Concerning siderophore activity, our proteomic data reveal that siderophore-associated proteins were reduced in both Δ*pglL* and ΔOGC strains (Fig. 2), with glycosylation-null strains producing reduced zones of clearing in the CAS assays (Fig. 4B and C; Fig. S5C and D). However, the magnitude of the reduction in the CAS assays differed in the mutant, since ΔOGC and Δ*pglL* ΔOGC strains presented significantly smaller zones of clearing than the Δ*pglL* strain (Fig. S5C and D). These results highlight that although the proteome changes observed in the Δ*pglL* and ΔOGC glycosylation mutants are highly similar, they are not identical and show phenotypic differences. Therefore, a key question arising from our findings is how the loss of glycosylation alters gene regulation and whether the observed defects are simply the result of altered transcriptional control. The lack of any glycosylated signaling/receptor-associated proteins in *B. cenocepacia* (56) makes the identification of the link between a specific glycoprotein and transcriptional control unclear.

It is possible the observed alterations in biofilm formation and siderophore activity are not solely driven by altered CepR regulation, but also reflect additional transcriptional alterations in the glycosylation-null strains. This conclusion agrees with our observations of many differences in the abundance of transcriptional regulators in the DNA-associated proteome of glycosylation-null strains (Fig. 3C; Data Set S1, tab 4). Further, biofilm formation within *B. cenocepacia* is modulated by multiple transcriptional regulators (33), making CepR just one of a range of regulators that could be driving this phenotype. An additional driver of these pleiotropic effects may also be deleterious outcomes resulting from the manipulation of the *O*-linked glycosylation system. It has been suggested in *C. jejuni* that the disruption of glycosylation leads to undecaprenyl diphosphate decorated with *N*-linked glycan being sequestered from the general undecaprenyl diphosphate pool and that this depot effect may be a general phenomenon observed in all glycosylation mutants (64). Sequestration of undecaprenyl diphosphate was thought to drive an increase in the abundance of proteins in the nonmevalonate and undecaprenyl diphosphate biosynthesis pathways observed in glycosylation-null *C. jejuni* (64). However, in *B. cenocepacia* glycosylation mutants, we observe only minor alterations in the nonmevalonate (BCAL0802, BCAL1884, BCAL2015, BCAL2016, BCAL2085, BCAL2710, BCAM0911 and BCAM2738 [see Fig. S6A in the supplemental material]) and undecaprenyl diphosphate biosynthesis (BCAL2087 and BCAM2067 [Fig. S6B]) pathways, which argues against this phenomenon being common to all glycosylation mutants. Furthermore, the similarity of the proteome changes in the Δ*pglL*, ΔOGC, and Δ*pglL* ΔOGC strains (Fig. S2C) supports the conclusion that proteome changes are independent of the sequestration of the undecaprenyl diphosphate pool as ΔOGC and Δ*pglL* ΔOGC strains are unable build the *O*-linked glycan on undecaprenyl diphosphate. Although our proteomic analysis shows similar protein levels across glycosylation-null and -competent strains, it is important to note that we have previously shown the loss of glycosylation reduces tolerance to oxidative and osmotic stresses (65). This suggests that additional off-target effects relating to lipid-linked glycan or membrane stress may occur that are driven by changes independent of protein abundance, such as changes in protein-protein interactions, protein localization, or protein folding.

Another explanation for the pleiotropic effects associated with loss of *O*-glycosylation could be the instability of the glycoproteins in the absence of the glycan. We identified two glycoproteins BCAL2974 and BCAL1086, both of unknown functions, which are reduced in abundance due to the loss of glycosylation. However, genetic experiments demonstrate that neither protein is responsible for the phenotypic and

proteomic changes associated with loss of glycosylation (Fig. 6 and 7). Furthermore, in the case of BCAL1086, endogenous tagging and degradomic analysis confirm the loss of this protein in the $\Delta pglL$ background. Although these results support the breakdown of BCAL1086 as a consequence of the loss of glycosylation, an alternative explanation is that the changes in degradation arise from alterations in protease levels or activities in the $\Delta pglL$ mutant. Previously, we reported that $\Delta pglL$ results in enhanced casein proteolytic activity (65). However, our global proteome analysis shows only modest changes in protease levels. We also observed identical protease profiles from activity probe against multiple classes of protease in the wild-type, $\Delta pglL$, and $\Delta pglL$ $amrAB$::S7-$pglL$-His$_{10}$ (Fig. S6C), suggesting all of these strains have similar protease activities. More importantly, aside from glycoproteins BCAL2974 and BCAL1086, the other proteins targeted for glycosylation remain consistently stable in the glycosylation-defective mutants. Although 23 glycoproteins are known in $B.$ $cenocepacia$, additional glycoproteins may also exist that were missed in the initial characterization of $B.$ $cenocepacia$ glycoproteome. Regardless, although loss of glycosylation may affect the stability of some glycoproteins, the pleiotropic effect found in the glycosylation mutants cannot be explained by alterations in protein degradation.

In summary, this work provides a global analysis of the effect of O-linked glycosylation on $B.$ $cenocepacia$ traits. The application of quantitative proteomics enabled the assessment of nearly half the predicted proteome of $B.$ $cenocepacia$ K56-2 and revealed a previously unknown link between O-linked glycosylation and transcriptional alterations. The alteration in known transcriptional regulators, such as CepR, as well as its associated phenotypes, supports a model in which the defects observed for glycosylation-null strains arise from transcriptional changes and not from the direct result of glycosylation loss per se. This work challenges the idea that loss of glycosylation solely affects the stability and activity of the glycoproteome and instead shows that glycosylation can influence the bacterial transcriptional profile and broader proteome.

MATERIALS AND METHODS

Bacterial strains and growth conditions. The strains and plasmids used in this study are listed in Tables 1 and 2, respectively. Strains of $Escherichia$ $coli$ and $B.$ $cenocepacia$ were grown at 37°C in Luria-Bertani (LB) medium. When required, antibiotics were added to the following final concentrations: 50 μg/ml trimethoprim for $E.$ $coli$ and 100 μg/ml for $B.$ $cenocepacia$, 20 μg/ml tetracycline for $E.$ $coli$ and 150 μg/ml for $B.$ $cenocepacia$, and 40 μg/ml kanamycin for $E.$ $coli$. Ampicillin was used at 100 μg/ml and polymyxin B at 25 μg/ml for triparental mating to select against donor and helper $E.$ $coli$ strains. Antibiotics were purchased from Thermo Fisher Scientific, while all other chemicals unless otherwise stated were provided by Sigma-Aldrich.

Recombinant DNA methods. The oligonucleotides used in this study are listed in Table 3. DNA ligations, restriction endonuclease digestions, and agarose gel electrophoresis were performed using standard molecular biology techniques (81), with Gibson assembly undertaken according to published protocols (82). All restriction enzymes, T4 DNA ligase, and Gibson master mix were used as recommended by the manufacturer (New England Biolabs). $E.$ $coli$ PIR2 and DH5α cells were transformed using heat shock-based transformation. PCR amplifications were carried out using either Phusion DNA (Thermo Fisher Scientific) or Pfu Ultra II (Agilent) polymerases were used according to the manufacturer's recommendations with the addition of 2.5% dimethyl sulfoxide (DMSO) for the amplification of $B.$ $cenocepacia$ DNA due to its high GC content. DNA isolation, PCR recoveries, and restriction digest purifications were performed using the genomic DNA cleanup kit (Zmyo Research, CA) or Wizard SV gel and PCR cleanup system (Promega). Colony and screening PCRs were performed using GoTaq Taq polymerase (Qiagen) supplemented with 10% DMSO when screening $B.$ $cenocepacia$. All constructs in Table 2 were confirmed by Sanger sequencing undertaken at the Australian Genome Research Facility (Melbourne, Australia).

Construction of unmarked deletion mutants, endogenous tagged BCAL1086, and complementation with $pglL$-His$_{10}$. Deletions and endogenous tagging of BCAL1086 were undertaken using the approach of Flannagan et al. for the construction of unmarked, nonpolar deletions in $B.$ $cenocepacia$ K56-2 (83). Chromosomal complements of $pglL$ were generated by introducing $pglL$-His$_{10}$ under the control of the $B.$ $cenocepacia$ S7 promoter (P_{S7}) or the native $pglL$ promoter (Ppgl; 660 bp upstream of PglL) inserted into $amrAB$ using the pMH447 (23) derivative plasmids (Table 2) according to the protocol of Aubert et al. (84).

Protein manipulation and immunoblotting. Bacterial whole-cell lysates were prepared from overnight LB cultures of $B.$ $cenocepacia$ strains. One milliliter of bacteria at an optical density at 600 nm (OD$_{600}$) of 1.0 were pelleted, then resuspended in a mixture of 4% sodium dodecyl sulfate (SDS), 100 mM Tris (pH 8.0), and 20 mM dithiothreitol (DTT) and boiled at 95°C with shaking at 2,000 rpm for 10 min.

TABLE 1 Strains used in this study

Strain	Description	Source
E. coli		
DH5α	F$^-$ ϕ80*lacZ*ΔM15 *endA1 recA1 hsdR17*(r$_K^-$ m$_K^+$) *phoA supE44 thi-1* ΔgyrA96 (Δ*lacZYA-argF*)U169 *relA1F* λ$^-$	Invitrogen
PIR2	F$^-$ Δ*lac169 rpoS*(Am) *robA1 creC510 hsdR514 endA recA1 uidA*(ΔMluI):: *pir-116*	Thermo Scientific
B. cenocepacia		
K56-2	Clinical isolate of the ET12 lineage[a]	Canadian *B. cepacia* Research and Referral Repository
K56-2 Δ*pglL*	Δ*pglL* (*BCAL0960*) derivative of K56-2 created using pYM8	This study
K56-2 ΔOGC	ΔOGC (*BCAL3114–BCAL3118*) derivative of K56-2 created using pGPi-SceI-OGC	This study
K56-2 Δ*pglL amrAB*::S7-*pglL*-His$_{10}$	*amrAB*::S7-*pglL*-His$_{10}$ chromosomal complement derivative of Δ*pglL* (*BCAL0960*) mutant created using pMH447-S7-*pglL*-His$_{10}$, gentamicin-sensitive strain	This study
K56-2 Δ*pglL amrAB*::native -*pglL*-His$_{10}$	*amrAB*::native *pglL* promoter-*pglL*-His$_{10}$ chromosomal complement derivative of Δ*pglL* (*BCAL0960*) mutant created using pMH447-native-*pglL*-His$_{10}$, gentamicin-sensitive strain	This study
K56-2 *BCAL1086*-His$_{10}$	Chromosomally tagged *BCAL1086* with a C-terminal His$_{10}$	This study
K56-2 Δ*pglL BCAL1086*-His$_{10}$	Δ*pglL* (*BCAL0960*) mutant derivative of K56-2, chromosomally tagged *BCAL1086* with a C-terminal His$_{10}$	This study
K56-2 Δ*pglL amrAB*::S7-*pglL*-His$_{10}$ *BCAL1086*-His$_{10}$	*amrAB*::S7-*pglL*-His$_{10}$ chromosomal complement derivative of Δ*pglL* (*BCAL0960*) mutant with a chromosomally tagged *BCAL1086* with a C-terminal His$_{10}$	This study
K56-2 Δ*BCAL1086*	Δ*BCAL1086* derivative of K56-2 created using pGPi-SceI-*BCAL1086*	This study
K56-2 Δ*BCAL2974*	Δ*BCAL2974* derivative of K56-2 created using pGPi-SceI-*BCAL2974*	This study
K56-2 Δ*cepR*	Δ*cepR* derivative of K56-2 created using pGPi-SceI-*cepR*	This study
K56-2 Δ*cepI*	Δ*cepI* derivative of K56-2 created using pGPi-SceI-*cepI*	This study

[a]See references 4 and 104 for details.

Samples were then mixed with Laemmli loading buffer (24.8 mM Tris, 10 mM glycerol, 0.5% [wt/vol] SDS, 3.6 mM β-mercaptoethanol, and 0.001% [wt/vol] bromophenol blue [pH 6.8], final concentration) and heated for a further 5 min at 95°C. Lysates were then subjected to SDS-PAGE using precast 4 to 12% gels (Invitrogen) and transferred to nitrocellulose membranes. Membranes were blocked for 1 h in 5% skim milk in TBS-T (20 mM Tris, 150 mM NaCl and 0.1% Tween 20) and then incubated for at least 16 h at 4°C with either mouse monoclonal anti-His (AD1.1.10, 1:2,000 [AbD Serotech]) or mouse anti-RNA pol (4RA2, 1:5,000 [Neoclone]). Proteins were detected using anti-mouse IgG horseradish peroxidase (HRP)-conjugated secondary antibodies (1:3,000 [Perkin-Elmer catalog no. NEF822001EA]) and developed with Clarity Western ECL (enhanced chemiluminescence) substrate (Bio-Rad). All antibodies were diluted in TBS-T with 1% bovine serum albumin (BSA [Sigma-Aldrich]). Images were obtained using an MFChemiBis imaging station (DNR Bio-Imaging Systems) or an Amersham imager 600 (GE Life Sciences).

Proteomic analysis. Whole-proteome sample preparation was undertaken as previously described (65), while peptidomic and DNA binding proteome analysis were undertaken according to the approaches of Parker et al. (76) and Qin et al. (85), respectively. For nonpeptidomic samples, isolated protein preparations were digested as previously described (86) and cleaned up using homemade stage tips according to the protocol of Ishihama and Rappsilber (87, 88). Peptidomic samples were cleaned up using commercial tC$_{18}$ columns (Waters). Purified peptides were resuspended in buffer A* (2% acetonitrile [ACN], 0.1% trifluoroacetic acid) and separated using a two-column chromatography setup comprising a PepMap100 C$_{18}$ 20-mm by 75-μm trap and a PepMap C$_{18}$ 500-mm by 75-μm analytical column (Thermo Scientific). Data were acquired on either an Orbitrap Elite mass spectrometer (Thermo Scientific), an Orbitrap Fusion Lumos Tribrid mass spectrometer (Thermo Scientific), or a Q-exactive plus mass spectrometer (Thermo Scientific) and processed using MaxQuant (v1.5.5.1 or 1.5.3.30 [89]). Database searching was carried out against the reference *B. cenocepacia* strain J2315 (https://www.uniprot.org/proteomes/UP000001035) and the K56-2 Valvano (90) (http://www.uniprot.org/taxonomy/985076) proteomes. Proteomic data sets have been deposited into the ProteomeXchange Consortium via the PRIDE (91) partner repository. A complete description of each PRIDE data set is provided in Table 4. A complete description of all proteomic-associated methods is provided in Text S1 in the supplemental material.

Motility assays. Motility assays were conducted using semisolid motility agar consisting of LB infusion medium supplemented with 0.3% agar as previously described (56). Plates were inoculated using 2 μl of standardized (OD$_{600}$ of 0.5) overnight cultures of each strain. Motility zones were measured after 48 h of incubation at 37°C. Experiments were carried out in triplicate with 3 biological replicates of each strain.

Transcriptional analysis by luminescence assays. To assess transcriptional changes in CepR and CepI, *luxCDABE* reporter assays were performed using the *B. cenocepacia* K56–2 wild–type (WT), Δ*pglL*,

TABLE 2 Plasmids used in this study

Plasmid	Description	Reference(s)
pRK2013	ori_{colE1}, RK2 derivative, Kan^r mob^+ tra^+	105
pGPI-SceI	$oriR6K$ mob^+ ΩTp^r, including ISce-I restriction site	83
pDAI-SceI-SacB	ori_{pBBR1} Tet^r P_{dhfr} mob^+, expressing ISce-I and negative selection marker SacB	83, 106
pMH447	pGPI-SceI with fragments flanking $\Delta amrAB$ (BCAL1674–BCAL1675)	106
pYM8	pGPI-SceI with fragments flanking $pglL$ (BCAL0960)	65
pGPI-SceI-OGC	pGPI-SceI with fragments flanking OGC (BCAL3114–BCAL3118)	This study
pMH447-S7-$pglL$-His$_{10}$	pMH447 with S7 promoter driving expression of $pglL$-His$_{10}$ from Met11 of open reading frame BCAL0960	This study
pMH447-native-$pglL$-His$_{10}$	pMH447 with native $pglL$-His$_{10}$ promoter driving expression of $pglL$	This study
pGPI-SceI-BCAL1086	pGPI-SceI with fragments flanking BCAL1086 to generate ΔBCAL1086 mutant	This study
pGPI-SceI-BCAL2974	pGPI-SceI with fragments flanking BCAL2974 to generate ΔBCAL2874 mutant	This study
pGPI-SceI-cepR	pGPI-SceI with fragments flanking $cepR$ (BCAM1868) to generate $\Delta cepR$ mutant	This study
pGPI-SceI-cepI	pGPI-SceI with fragments flanking $cepI$ (BCAM1870) to generate $\Delta cepI$ mutant	This study
pGPI-SceI-BCAL1086-His$_{10}$	pGPI-SceI with fragments flanking BCAL1086 to generate BCAL1086-His$_{10}$ mutant	This study
pKM4	Tp^r pMLBad–based plasmid containing C-terminal His$_6$–tagged DsbA1 from *Neisseria meningitidis* MC58	66
pMS402	Promoterless $luxCDABE$ promoter reporter plasmid, Kan^r Tp^r	92
pPromcepR	$cepR$::$luxCDABE$ transcriptional fusion in pMS402, Kan^r Tp^r	69
pCP300	$cepI$::$luxCDABE$ transcriptional fusion in pMS402, Kan^r Tp^r	72

ΔOGC, and Δ$pglL$ $amrAB$::S7-$pglL$-His$_{10}$ strains containing pCP300 (CepI promoter $luxCDABE$ reporter [72]), pPromcepR (CepR promoter $luxCDABE$ reporter [69]) or pMS402 (promoterless $luxCDABE$ reporter [92]) as a negative control. Overnight cultures were diluted to an OD$_{600}$ of 1.0, and 2 μl was inoculated into 200 μl LB supplemented with 100 μg/ml trimethoprim in black, clear–bottom 96–well microplates (minimum of eight technical replicates per independent biological replicate). The OD$_{600}$ and relative luminescence were measured using a CLARIOstar plate reader at 10-min intervals for 24 h. Experiments assessing the effect of C$_8$-HSL additions on CepR and CepI transcription were performed according to Le Guillouzer et al. (93). Briefly, cultures were supplemented with C$_8$-HSL (Sigma-Aldrich) resuspended in acetonitrile (10 μM final concentration) and added to cultures with acetonitrile added alone used as a negative control. Plates were incubated at 37°C with shaking at 200 rpm between measurements, with each assay undertaken 3 independent times on separate days. The resulting outputs were visualized using R (https://www.r-project.org/).

Biofilm assay. Biofilm assays were performed according to previous reports (26, 94, 95) using protocols based on the approach of O'Toole (96). *B. cenocepacia* strains were grown overnight at 37°C and adjusted to an OD$_{600}$ of 1.0. Ten microliters of these suspensions was inoculated into 990 μl of LB supplemented with 0.5% (wt/vol) Casamino Acids, and 100 μl was added into 96-well microtiter plates (Corning Life Sciences [a minimum of eight technical replicates per independent biological replicate]). Microtiter plates were incubated at 37°C for 24 h in a closed humidified plastic container. The plates were then washed with phosphate-buffered saline (PBS) to remove planktonic cells then stained for 15 min with 125 μl of 1% (wt/vol) crystal violet. Excess crystal violet was removed with two washes of PBS and 200 μl of 33% (vol/vol) acetic acid was added for 15 min to release the stain. The resuspended stain was transferred to a new plate and measured on a CLARIOstar plate reader measuring the absorbance of the resulting solution at 595 nm. Three independent assays were undertaken on separate days.

Galleria mellonella infection assays. Infection of *G. mellonella* larvae was undertaken using the approach of Seed and Dennis (97) with minor modifications. *B. cenocepacia* strains were grown overnight at 37°C and adjusted to an OD$_{600}$ of 1.0, equivalent to 2×10^9 CFU/ml. Strains were diluted with PBS to 4×10^5 CFU/ml, with serial dilution plates undertaken to confirm inoculum levels. For each strain, 2,000 CFU in 5 μl was injected in the right proleg of the *G. mellonella* larvae. Three independent challenges were performed with each strain injected into 8 to 10 *G. mellonella* larvae. For each independent challenge, 8 control larvae were injected with 5 μl PBS. Postinfection, *G. mellonella* larvae were placed in

TABLE 3 Primers used in this study

Primer	Sequence[a]	Description	Restriction site[b]
NS01	AAA<u>TCTAGA</u>GTGACGACGATGCACGAAT	*BCAL3114* (*ogcX*) forward	XbaI
NS02	AAA<u>CTCGAG</u>AAATTAATTTAATTGATCTGGGTGAGCCGTTC	*BCAL3114* (*ogcX*) reverse	XhoI
NS03	AAA<u>CTCGAG</u>AATAAGCTTCATCGTCTCCCTGCT	*BCAL3118* (*ogcI*) forward	XhoI
NS04	AAA<u>CCCGGG</u>GAAGCAGGTCTCGAAGATCG	*BCAL3118* (*ogcI*) reverse	SmaI
NS05	AAA<u>CCCGGG</u>GCCTACGTGATCTTCCACGA	*BCAL0230* (S7) promoter forward for *pglL* cloning	SmaI
NS06	CGAACGGGAAAAGTAGAAGGCATGATTCTTCCTTTACTTGTTCAGTTGGAGC	*BCAL0230* (S7) promoter reverse for *pglL* cloning from Met11	—
NS07	GCTCCAACTGAACAAGTAAAGGAAGAATCATGCCTTCTACTTTTTCCCGTTCG	*BCAL0960* (*pglL*) forward amplifying from Met11	—
NS08	AAA<u>CCCGGG</u>TCAGTGGTGGTGGTGGTGGTGGTGGTGGTGATCCGAATCGTCGTCGTCCG	*BCAL0960* (*pglL*) reverse with His$_{10}$ tag	SmaI
NS09	GGAATTTCACGACATGGCCCGCAAGACCCTTCACGCTGATCGAACTGAT	*BCAL0960* (*pglL*) with native promoter forward	—
NS10	CCGGTGCTTGATGGCGAGCGATTCTTCCCTCAGTGGTGGTGGTGGTGGTGGTGGTGGTGATCCGAATCGTCGTCGTCCG	*BCAL0960* (*pglL*) with native promoter reverse	—
NS11	TTTT<u>GAATTC</u>GCGTTCGAGGTACCAGTCC	*BCAM1868* (*cepR*) upstream forward	EcoRI
NS12	TTTT<u>GTCGAC</u>CCCGAGCCGCTTGAATAG	*BCAM1868* (*cepR*) upstream reverse	SalI
NS13	TTTT<u>GTCGAC</u>TCCACGTGAACAACATCCTC	*BCAM1868* (*cepR*) downstream forward	SalI
NS14	TTTT<u>TCTAGA</u>CTGCTCACCAATACGGTGCT	*BCAM1868* (*cepR*) downstream reverse	XbaI
NS15	TTTA<u>TCTAGA</u>CTGGGACTGGTACCTCGAAC	*BCAM1870* (*cepI*) upstream forward	XbaI
NS16	TTTT<u>CTCGAG</u>AGGTCTGCATGGATGTCCTC	*BCAM1870* (*cepI*) upstream reverse	XhoI
NS17	TTTT<u>CTCGAG</u>AGGTAGATGGGCGTCTGGT	*BCAM1870* (*cepI*) downstream forward	XhoI
NS18	TTTA<u>GAATTC</u>CTGCATCGTCAGGTCGTG	*BCAM1870* (*cepI*) downstream reverse	EcoRI
NS19	AAAA<u>CTCGAG</u>CTATCGATCGCGTCTTCGTTAC	*BCAL2974* upstream reverse	XhoI
NS20	AAAA<u>TCTAGAG</u>CCACGTGCTGATTCATCT	*BCAL2974* upstream forward	XbaI
NS21	AAAA<u>GAATTC</u>CTGGATCGCTTCCGGATAAT	*BCAL2974* downstream forward	EcoRI
NS22	AAAA<u>CTCGAG</u>GAAATACCAGGGCAGCAAGA	*BCAL2974* downstream reverse	XhoI
NS23	AAAA<u>CTCGAG</u>GCAAGAAACTCCAGCAGTGG	*BCAL1086* downstream forward	XhoI
NS24	AAAA<u>GAATTC</u>ATTCAATGAACGTTGCGTCA	*BCAL1086* downstream reverse	EcoRI
NS25	AAAA<u>TCTAGA</u>TGCGTACGACGAACGAAG	*BCAL1086* upstream forward	XbaI
NS26	AAAA<u>CTCGAG</u>CTACATGTTCATCAGCAATCTCCGG	*BCAL1086* upstream reverse	XhoI
NS27	AAAA<u>TCTAGA</u>TGCGATTGAATCAGACGAAT	*BCAL1086* His$_{10}$ tagging upstream forward	XbaI
NS28	TCAGTGGTGGTGGTGGTGGTGGTGGTGGTGTTCACCGCTCGCGGGTTTGGCC	*BCAL1086* His$_{10}$ tagging upstream reverse	—
NS29	CCACCACCACCACCACCACTGACGCGGGCTTGCACGATCCGC	*BCAL1086* His$_{10}$ tagging downstream forward	—
NS30	AAAA<u>TCTAGA</u>CTCCAGATCCAGCATGTCG	*BCAL1086* His$_{10}$ tagging downstream reverse	XbaI

[a]Restriction sites are underlined when present.
[b]—, primer for Gibson assembly or overlap PCR.

12-well tissue culture plates and incubated in the dark at 30°C. The number of dead larvae was scored at 24, 48, and 72 h after infection, with death of the larvae determined by loss of responsiveness to touch. The results visualized using R (https://www.r-project.org/), and statistical analysis of survival curves was undertaken with the survminer package (version 0.4.5).

CAS siderophore assays. Alterations in activities of siderophores were assessed using the chrome azurol S (CAS) assay as previously described (98, 99). Ten microliters of adjusted bacterial culture at an OD_{600} of 1.0 was spotted on CAS agar plates and incubated at 37°C for 24 h. The diameter of the zone of discoloration from the removal of iron from the CAS dye complex was measured. Experiments were carried out with at least 3 biological replicates in technical triplicate.

Protease activity-based probes. K56-2 WT, Δ*pglL*, and Δ*pglL amrAB*::S7-*pglL*-His$_{10}$ strains were grown overnight on confluent LB plates. Plates were flooded with 5 ml of prechilled sterile PBS, and colonies were removed with a cell scraper. Cells were washed 3 times in chilled PBS and resuspend in 40 mM Tris–150 mM NaCl (pH 7.8) and then lysed by sonication. Samples were clarified by centrifugation at 10,000 × *g* for 10 min at 4°C, and samples were diluted to a total concentration of 4 mg/ml. Reactivity to three classes of activity-based probes was assessed using PK-DPP (Cy5-tagged probe for trypsin-like proteases [100]), PK105b (Cy5-tagged probe for elastase-like proteases [101]), PK101 (biotin-tagged probe for elastase-like proteases [102]), and FP-biotin (biotin-tagged probe for serine hydrolases [103]), which were added at 1.3 μM from a 100× DMSO stock. Untreated control samples were prepared in parallel and left untreated to allow the assessment of autofluorescence and endogenous biotinylation in lysates. Samples were incubated at 37°C for 15 min to allow labeling and then quenched by the addition of Laemmli sample buffer. Samples were then boiled, and proteins were resolved on a 15% SDS-PAGE gel. For Cy5-tagged probes, labeling was detected by directly scanning the gel for Cy5 fluorescence using a Typhoon 5 flatbed laser scanner (GE Healthcare). For FP-biotin, proteins were transferred to nitrocellulose and the membrane was incubated with streptavidin-Alexa Fluor 647 at 4°C overnight. Following three washes with PBS containing 0.05% Tween 20, the membrane was scanned on the Typhoon 5 in the

TABLE 4 Description of proteomic experiments within PRIDE repository[a]

PRIDE accession no.	Title	Description
PXD014614	Peptidomic analysis of *B. cenocepacia* strains	Comparison of endogenous peptide pool in *B. cenocepacia* K56-2 strains to identify evidence for glycoprotein degradation in the absence of glycosylation; strains used are K56-2 WT, Δ*pglL* mutant, and Δ*pglL amrAB*::S7-*pglL*-His$_{10}$ complemented strain; LFQ-based quantification undertaken using Maxquant with 4 biologicals of each strain type
PXD014581	LFQ *B. cenocepacia* mutant comparison	Comparison of multiple *B. cenocepacia* K56-2 mutants to assess proteome changes; 7-strain comparison between the K56-2 WT, Δ*pglL*, Δ*BCAL*1086, Δ*BCAL*2974, Δ*cepI*, Δ*cepR* and Δ*pglL* mutants, and *amrAB*::S7-*pglL*-His$_{10}$ complemented strain; LFQ-based quantification undertaken using Maxquant with 5 biologicals of each strain type
PXD014516	LFQ *B. cenocepacia* Δ*pglL* mutant comparison	Characterization of the effect of *pglL* mutants and complement in *B. cenocepacia* K56-2; 6-strain comparison of K56-2 WT, Δ*pglL* (independent mutant 1), Δ*pglL* (independent mutant 2), Δ*pglL* (independent mutant 1) *amrAB*::native-*pglL*-His$_{10}$, Δ*pglL* (independent mutant 1) *amrAB*::S7-*pglL*-His$_{10}$, and Δ*pglL* (independent mutant 2) *amrAB*::native-*pglL*-His$_{10}$ strains; LFQ-based quantification with 4 biologicals of each strain type
PXD014429	LFQ *B. cenocepacia* glycosylation mutant comparison	Characterization of effect of glycosylation disruption in *B. cenocepacia* K56-2; 5-strain comparison of K56-2 WT, Δ*pglL*, ΔOGC, Δ*pglL* ΔOGC, and Δ*pglL amrAB*::S7-*pglL*-His$_{10}$ strains; LFQ-based quantification undertaken using Maxquant with 5 biologicals of each strain type
PXD014700	LFQ *B. cenocepacia* comparison of DNA binding proteome	Comparison of alterations in the DNA-bound proteome of *B. cenocepacia* K56-2 mutants. DDA experiments undertaken using 4 strains; K56-2 WT, Δ*pglL*, ΔOGC, and Δ*pglL amrAB*::S7-*pglL*-His$_{10}$ strains used for DDA experiments, while K56-2 WT, Δ*pglL*, and Δ*pglL amrAB*::S7-*pglL*-His$_{10}$ strains used for DIA experiments; LFQ-based quantification undertaken using Maxquant with four biologicals of each strain type

[a]All proteomic data in this study have been uploaded to the PRIDE proteomic repository and are accessible through the corresponding accession numbers. LFQ, label-free quantification; DDA, data-dependent acquisition; DIA, data-independent acquisition.

Cy5 channel. Experiments were carried out in biological triplicate. All probes were synthesized in-house by the Edgington-Mitchell Laboratory according to published methods, with the exception of FP-biotin, which was purchased from Santa Cruz Biotechnology.

Data availability. Proteomic data sets have been deposited into the ProteomeXchange Consortium via the PRIDE (91) partner repository with the data set identifiers PXD014429, PXD014516, PXD014581, PXD014614, and PXD014700.

SUPPLEMENTAL MATERIAL

Supplemental material for this article may be found at https://doi.org/10.1128/mSphere.00660-19.

TEXT S1, DOCX file, 0.1 MB.
FIG S1, TIF file, 1.2 MB.
FIG S2, EPS file, 1.2 MB.
FIG S3, TIF file, 1.6 MB.
FIG S4, TIF file, 1.3 MB.
FIG S5, TIF file, 1.1 MB.
FIG S6, TIF file, 1.3 MB.
TABLE S1, XLSX file, 0.1 MB.
DATA SET S1, XLSX file, 6.4 MB.

REFERENCES

1. Vanlaere E, Baldwin A, Gevers D, Henry D, De Brandt E, LiPuma JJ, Mahenthiralingam E, Speert DP, Dowson C, Vandamme P. 2009. Taxon K, a complex within the Burkholderia cepacia complex, comprises at least two novel species, Burkholderia contaminans sp. nov. and Burkholderia lata sp. nov. Int J Syst Evol Microbiol 59:102–111. https://doi .org/10.1099/ijs.0.001123-0.

2. De Smet B, Mayo M, Peeters C, Zlosnik JE, Spilker T, Hird TJ, LiPuma JJ, Kidd TJ, Kaestli M, Ginther JL, Wagner DM, Keim P, Bell SC, Jacobs JA, Currie BJ, Vandamme P. 2015. Burkholderia stagnalis sp. nov. and Burkholderia territorii sp. nov., two novel Burkholderia cepacia complex species from environmental and human sources. Int J Syst Evol Microbiol 65:2265–2271. https://doi.org/10.1099/ijs.0.000251.

3. Ong KS, Aw YK, Lee LH, Yule CM, Cheow YL, Lee SM. 2016. Burkholderia paludis sp. nov., an antibiotic-siderophore producing novel Burkholderia cepacia complex species, isolated from Malaysian tropical peat swamp soil. Front Microbiol 7:2046. https://doi.org/10.3389/fmicb.2016 .02046.

4. Mahenthiralingam E, Urban TA, Goldberg JB. 2005. The multifarious, multireplicon Burkholderia cepacia complex. Nat Rev Microbiol 3:144–156. https://doi.org/10.1038/nrmicro1085.

5. Loutet SA, Valvano MA. 2010. A decade of Burkholderia cenocepacia virulence determinant research. Infect Immun 78:4088–4100. https:// doi.org/10.1128/IAI.00212-10.

6. Huang CH, Jang TN, Liu CY, Fung CP, Yu KW, Wong WW. 2001. Characteristics of patients with Burkholderia cepacia bacteremia. J Microbiol Immunol Infect 34:215–219.

7. Hanulik V, Webber MA, Chroma M, Uvizl R, Holy O, Whitehead RN, Baugh S, Matouskova I, Kolar M. 2013. An outbreak of Burkholderia multivorans beyond cystic fibrosis patients. J Hosp Infect 84:248–251. https://doi.org/10.1016/j.jhin.2013.04.001.

8. Liao CH, Chang HT, Lai CC, Huang YT, Hsu MS, Liu CY, Yang CJ, Hsueh PR. 2011. Clinical characteristics and outcomes of patients with Burkholderia cepacia bacteremia in an intensive care unit. Diagn Microbiol Infect Dis 70:260–266. https://doi.org/10.1016/j.diagmicrobio.2011.01 .008.

9. Regan KH, Bhatt J. 2019. Eradication therapy for Burkholderia cepacia complex in people with cystic fibrosis. Cochrane Database Syst Rev 4:CD009876. https://doi.org/10.1002/14651858.CD009876.pub4.

10. Govan JR, Brown PH, Maddison J, Doherty CJ, Nelson JW, Dodd M, Greening AP, Webb AK. 1993. Evidence for transmission of Pseudomonas cepacia by social contact in cystic fibrosis. Lancet 342:15–19. https://doi.org/10.1016/0140-6736(93)91881-l.

11. Fung SK, Dick H, Devlin H, Tullis E. 1998. Transmissibility and infection control implications of Burkholderia cepacia in cystic fibrosis. Can J Infect Dis 9:177–182. https://doi.org/10.1155/1998/269157.

12. Ledson MJ, Gallagher MJ, Jackson M, Hart CA, Walshaw MJ. 2002. Outcome of Burkholderia cepacia colonisation in an adult cystic fibrosis centre. Thorax 57:142–145. https://doi.org/10.1136/thorax.57.2.142.

13. Chaparro C, Maurer J, Gutierrez C, Krajden M, Chan C, Winton T, Keshavjee S, Scavuzzo M, Tullis E, Hutcheon M, Kesten S. 2001. Infection with Burkholderia cepacia in cystic fibrosis: outcome following lung transplantation. Am J Respir Crit Care Med 163:43–48. https://doi.org/ 10.1164/ajrccm.163.1.9811076.

14. Horsley A, Webb K, Bright-Thomas R, Govan J, Jones A. 2011. Can early Burkholderia cepacia complex infection in cystic fibrosis be eradicated with antibiotic therapy? Front Cell Infect Microbiol 1:18. https://doi.org/ 10.3389/fcimb.2011.00018.

15. Kidd TJ, Douglas JM, Bergh HA, Coulter C, Bell SC. 2008. Burkholderia cepacia complex epidemiology in persons with cystic fibrosis from Australia and New Zealand. Res Microbiol 159:194–199. https://doi.org/ 10.1016/j.resmic.2008.01.001.

16. Reik R, Spilker T, Lipuma JJ. 2005. Distribution of Burkholderia cepacia complex species among isolates recovered from persons with or without cystic fibrosis. J Clin Microbiol 43:2926–2928. https://doi.org/10 .1128/JCM.43.6.2926-2928.2005.

17. Kenna DTD, Lilley D, Coward A, Martin K, Perry C, Pike R, Hill R, Turton JF. 2017. Prevalence of Burkholderia species, including members of Burkholderia cepacia complex, among UK cystic and non-cystic fibrosis patients. J Med Microbiol 66:490–501. https://doi.org/10.1099/jmm.0 .000458.

18. Lupo A, Isis E, Tinguely R, Endimiani A. 2015. Clonality and antimicrobial susceptibility of Burkholderia cepacia complex isolates collected from cystic fibrosis patients during 1998–2013 in Bern, Switzerland. New Microbiol 38:281–288.

19. De Soyza A, McDowell A, Archer L, Dark JH, Elborn SJ, Mahenthiralingam E, Gould K, Corris PA. 2001. Burkholderia cepacia complex genomovars and pulmonary transplantation outcomes in patients with cystic fibrosis. Lancet 358:1780–1781. https://doi.org/10.1016/S0140 -6736(01)06808-8.

20. Gilchrist FJ, Webb AK, Bright-Thomas RJ, Jones AM. 2012. Successful treatment of cepacia syndrome with a combination of intravenous cyclosporin, antibiotics and oral corticosteroids. J Cyst Fibros 11: 458–460. https://doi.org/10.1016/j.jcf.2012.04.002.

21. Jassem AN, Zlosnik JE, Henry DA, Hancock RE, Ernst RK, Speert DP. 2011. In vitro susceptibility of Burkholderia vietnamiensis to aminoglycosides. Antimicrob Agents Chemother 55:2256–2264. https://doi.org/10.1128/ AAC.01434-10.

22. Malott RJ, Steen-Kinnaird BR, Lee TD, Speert DP. 2012. Identification of hopanoid biosynthesis genes involved in polymyxin resistance in Burkholderia multivorans. Antimicrob Agents Chemother 56:464–471. https://doi.org/10.1128/AAC.00602-11.

23. Hamad MA, Skeldon AM, Valvano MA. 2010. Construction of aminoglycoside-sensitive Burkholderia cenocepacia strains for use in studies of intracellular bacteria with the gentamicin protection assay. Appl Environ Microbiol 76:3170–3176. https://doi.org/10.1128/AEM.03024-09.

24. Coenye T. 2010. Social interactions in the Burkholderia cepacia complex: biofilms and quorum sensing. Future Microbiol 5:1087–1099. https://doi.org/10.2217/fmb.10.68.

25. Van Acker H, Van Dijck P, Coenye T. 2014. Molecular mechanisms of antimicrobial tolerance and resistance in bacterial and fungal biofilms. Trends Microbiol 22:326–333. https://doi.org/10.1016/j.tim .2014.02.001.

26. Conway BA, Venu V, Speert DP. 2002. Biofilm formation and acyl homoserine lactone production in the Burkholderia cepacia complex. J Bacteriol 184:5678–5685. https://doi.org/10.1128/jb.184.20 .5678-5685.2002.

27. Savoia D, Zucca M. 2007. Clinical and environmental Burkholderia strains: biofilm production and intracellular survival. Curr Microbiol 54:440–444. https://doi.org/10.1007/s00284-006-0601-9.

28. Schwab U, Leigh M, Ribeiro C, Yankaskas J, Burns K, Gilligan P, Sokol P, Boucher R. 2002. Patterns of epithelial cell invasion by different species of the Burkholderia cepacia complex in well-differentiated human airway epithelia. Infect Immun 70:4547–4555. https://doi.org/10.1128/ iai.70.8.4547-4555.2002.

29. Schwab U, Abdullah LH, Perlmutt OS, Albert D, Davis CW, Arnold RR, Yankaskas JR, Gilligan P, Neubauer H, Randell SH, Boucher RC. 2014. Localization of Burkholderia cepacia complex bacteria in cystic fibrosis lungs and interactions with Pseudomonas aeruginosa in hypoxic mucus. Infect Immun 82:4729–4745. https://doi.org/10.1128/IAI.01876-14.

30. Sajjan U, Corey M, Humar A, Tullis E, Cutz E, Ackerley C, Forstner J. 2001. Immunolocalisation of Burkholderia cepacia in the lungs of cystic fibrosis patients. J Med Microbiol 50:535–546. https://doi.org/10.1099/0022-1317-50-6-535.

31. Cunha MV, Sousa SA, Leitao JH, Moreira LM, Videira PA, Sa-Correia I. 2004. Studies on the involvement of the exopolysaccharide produced by cystic fibrosis-associated isolates of the Burkholderia cepacia complex in biofilm formation and in persistence of respiratory infections. J Clin Microbiol 42:3052–3058. https://doi.org/10.1128/JCM.42.7.3052-3058.2004.

32. Traverse CC, Mayo-Smith LM, Poltak SR, Cooper VS. 2013. Tangled bank of experimentally evolved Burkholderia biofilms reflects selection during chronic infections. Proc Natl Acad Sci U S A 110:E250–E259. https://doi.org/10.1073/pnas.1207025110.

33. Suppiger A, Schmid N, Aguilar C, Pessi G, Eberl L. 2013. Two quorum sensing systems control biofilm formation and virulence in members of the Burkholderia cepacia complex. Virulence 4:400–409. https://doi.org/10.4161/viru.25338.

34. Baldwin A, Sokol PA, Parkhill J, Mahenthiralingam E. 2004. The Burkholderia cepacia epidemic strain marker is part of a novel genomic island encoding both virulence and metabolism-associated genes in Burkholderia cenocepacia. Infect Immun 72:1537–1547. https://doi.org/10.1128/iai.72.3.1537-1547.2004.

35. Malott RJ, O'Grady EP, Toller J, Inhülsen S, Eberl L, Sokol PA. 2009. A Burkholderia cenocepacia orphan LuxR homolog is involved in quorum-sensing regulation. J Bacteriol 191:2447–2460. https://doi.org/10.1128/JB.01746-08.

36. Lutter E, Lewenza S, Dennis JJ, Visser MB, Sokol PA. 2001. Distribution of quorum-sensing genes in the Burkholderia cepacia complex. Infect Immun 69:4661–4666. https://doi.org/10.1128/IAI.69.7.4661-4666.2001.

37. Gotschlich A, Huber B, Geisenberger O, Togl A, Steidle A, Riedel K, Hill P, Tummler B, Vandamme P, Middleton B, Camara M, Williams P, Hardman A, Eberl L. 2001. Synthesis of multiple N-acylhomoserine lactones is wide-spread among the members of the Burkholderia cepacia complex. Syst Appl Microbiol 24:1–14. https://doi.org/10.1078/0723-2020-00013.

38. Lewenza S, Conway B, Greenberg EP, Sokol PA. 1999. Quorum sensing in Burkholderia cepacia: identification of the LuxRI homologs CepRI. J Bacteriol 181:748–756.

39. Huber B, Riedel K, Hentzer M, Heydorn A, Gotschlich A, Givskov M, Molin S, Eberl L. 2001. The cep quorum-sensing system of Burkholderia cepacia H111 controls biofilm formation and swarming motility. Microbiology 147:2517–2528. https://doi.org/10.1099/00221287-147-9-2517.

40. Uehlinger S, Schwager S, Bernier SP, Riedel K, Nguyen DT, Sokol PA, Eberl L. 2009. Identification of specific and universal virulence factors in Burkholderia cenocepacia strains by using multiple infection hosts. Infect Immun 77:4102–4110. https://doi.org/10.1128/IAI.00398-09.

41. Chapalain A, Vial L, Laprade N, Dekimpe V, Perreault J, Deziel E. 2013. Identification of quorum sensing-controlled genes in Burkholderia ambifaria. Microbiologyopen 2:226–242. https://doi.org/10.1002/mbo3.67.

42. Sokol PA, Sajjan U, Visser MB, Gingues S, Forstner J, Kooi C. 2003. The CepIR quorum-sensing system contributes to the virulence of Burkholderia cenocepacia respiratory infections. Microbiology 149:3649–3658. https://doi.org/10.1099/mic.0.26540-0.

43. O'Grady EP, Viteri DF, Malott RJ, Sokol PA. 2009. Reciprocal regulation by the CepIR and CciIR quorum sensing systems in Burkholderia cenocepacia. BMC Genomics 10:441. https://doi.org/10.1186/1471-2164-10-441.

44. Subsin B, Chambers CE, Visser MB, Sokol PA. 2007. Identification of genes regulated by the cepIR quorum-sensing system in Burkholderia cenocepacia by high-throughput screening of a random promoter library. J Bacteriol 189:968–979. https://doi.org/10.1128/JB.01201-06.

45. Inhulsen S, Aguilar C, Schmid N, Suppiger A, Riedel K, Eberl L. 2012. Identification of functions linking quorum sensing with biofilm formation in Burkholderia cenocepacia H111. Microbiologyopen 1:225–242. https://doi.org/10.1002/mbo3.24.

46. Kooi C, Corbett CR, Sokol PA. 2005. Functional analysis of the Burkholderia cenocepacia ZmpA metalloprotease. J Bacteriol 187:4421–4429. https://doi.org/10.1128/JB.187.13.4421-4429.2005.

47. Kooi C, Subsin B, Chen R, Pohorelic B, Sokol PA. 2006. Burkholderia cenocepacia ZmpB is a broad-specificity zinc metalloprotease involved in virulence. Infect Immun 74:4083–4093. https://doi.org/10.1128/IAI.00297-06.

48. Lewenza S, Sokol PA. 2001. Regulation of ornibactin biosynthesis and N-acyl-L-homoserine lactone production by CepR in Burkholderia cepacia. J Bacteriol 183:2212–2218. https://doi.org/10.1128/JB.183.7.2212-2218.2001.

49. Nothaft H, Szymanski CM. 2013. Bacterial protein N-glycosylation: new perspectives and applications. J Biol Chem 288:6912–6920. https://doi.org/10.1074/jbc.R112.417857.

50. Szymanski CM, Wren BW. 2005. Protein glycosylation in bacterial mucosal pathogens. Nat Rev Microbiol 3:225–237. https://doi.org/10.1038/nrmicro1100.

51. Koomey M. 2019. O-linked protein glycosylation in bacteria: snapshots and current perspectives. Curr Opin Struct Biol 56:198–203. https://doi.org/10.1016/j.sbi.2019.03.020.

52. Fletcher CM, Coyne MJ, Villa OF, Chatzidaki-Livanis M, Comstock LE. 2009. A general O-glycosylation system important to the physiology of a major human intestinal symbiont. Cell 137:321–331. https://doi.org/10.1016/j.cell.2009.02.041.

53. Elhenawy W, Scott NE, Tondo ML, Orellano EG, Foster LJ, Feldman MF. 2016. Protein O-linked glycosylation in the plant pathogen Ralstonia solanacearum. Glycobiology 26:301–311. https://doi.org/10.1093/glycob/cwv098.

54. Harding CM, Nasr MA, Kinsella RL, Scott NE, Foster LJ, Weber BS, Fiester SE, Actis LA, Tracy EN, Munson RS, Jr, Feldman MF. 2015. Acinetobacter strains carry two functional oligosaccharyltransferases, one devoted exclusively to type IV pilin, and the other one dedicated to O-glycosylation of multiple proteins. Mol Microbiol 96:1023–1041. https://doi.org/10.1111/mmi.12986.

55. Iwashkiw JA, Seper A, Weber BS, Scott NE, Vinogradov E, Stratilo C, Reiz B, Cordwell SJ, Whittal R, Schild S, Feldman MF. 2012. Identification of a general O-linked protein glycosylation system in Acinetobacter baumannii and its role in virulence and biofilm formation. PLoS Pathog 8:e1002758. https://doi.org/10.1371/journal.ppat.1002758.

56. Lithgow KV, Scott NE, Iwashkiw JA, Thomson EL, Foster LJ, Feldman MF, Dennis JJ. 2014. A general protein O-glycosylation system within the Burkholderia cepacia complex is involved in motility and virulence. Mol Microbiol 92:116–137. https://doi.org/10.1111/mmi.12540.

57. Nothaft H, Scott NE, Vinogradov E, Liu X, Hu R, Beadle B, Fodor C, Miller WG, Li J, Cordwell SJ, Szymanski CM. 2012. Diversity in the protein N-glycosylation pathways within the Campylobacter genus. Mol Cell Proteomics 11:1203–1219. https://doi.org/10.1074/mcp.M112.021519.

58. Scott NE, Kinsella RL, Edwards AV, Larsen MR, Dutta S, Saba J, Foster LJ, Feldman MF. 2014. Diversity within the O-linked protein glycosylation systems of acinetobacter species. Mol Cell Proteomics 13:2354–2370. https://doi.org/10.1074/mcp.M114.038315.

59. Coyne MJ, Fletcher CM, Chatzidaki-Livanis M, Posch G, Schaffer C, Comstock LE. 2013. Phylum-wide general protein O-glycosylation system of the Bacteroidetes. Mol Microbiol 88:772–783. https://doi.org/10.1111/mmi.12220.

60. Posch G, Pabst M, Neumann L, Coyne MJ, Altmann F, Messner P, Comstock LE, Schaffer C. 2012. Cross-glycosylation" of proteins in Bacteriodales species. Glycobiology https://doi.org/10.1093/glycob/cws172.

61. Iwashkiw JA, Vozza NF, Kinsella RL, Feldman MF. 2013. Pour some sugar on it: the expanding world of bacterial protein O-linked glycosylation. Mol Microbiol 89:14–28. https://doi.org/10.1111/mmi.12265.

62. Nothaft H, Szymanski CM. 2010. Protein glycosylation in bacteria: sweeter than ever. Nat Rev Microbiol 8:765–778. https://doi.org/10.1038/nrmicro2383.

63. Cain JA, Dale AL, Niewold P, Klare WP, Man L, White MY, Scott NE, Cordwell SJ. 2019. Proteomics reveals multiple phenotypes associated with N-linked glycosylation in Campylobacter jejuni. Mol Cell Proteomics 18:715. https://doi.org/10.1074/mcp.RA118.001199.

64. Abouelhadid S, North SJ, Hitchen P, Vohra P, Chintoan-Uta C, Stevens M, Dell A, Cuccui J, Wren BW. 2019. Quantitative analyses reveal novel roles for N-glycosylation in a major enteric bacterial pathogen. mBio 10:e00297-19. https://doi.org/10.1128/mBio.00297-19.

65. Fathy Mohamed Y, Scott NE, Molinaro A, Creuzenet C, Ortega X, Lertmemongkolchai G, Tunney MM, Green H, Jones AM, DeShazer D, Currie BJ, Foster LJ, Ingram R, De Castro C, Valvano MA. 2019. A general protein O-glycosylation machinery conserved in Burkholderia species improves bacterial fitness and elicits glycan immunogenicity in hu-

mans. J Biol Chem 294:13248–13268. https://doi.org/10.1074/jbc.RA119.009671.

66. Gebhart C, Ielmini MV, Reiz B, Price NL, Aas FE, Koomey M, Feldman MF. 2012. Characterization of exogenous bacterial oligosaccharyltransferases in Escherichia coli reveals the potential for O-linked protein glycosylation in Vibrio cholerae and Burkholderia thailandensis. Glycobiology 22:962–974. https://doi.org/10.1093/glycob/cws059.

67. Chambers CE, Lutter EI, Visser MB, Law PP, Sokol PA. 2006. Identification of potential CepR regulated genes using a cep box motif-based search of the Burkholderia cenocepacia genome. BMC Microbiol 6:104. https://doi.org/10.1186/1471-2180-6-104.

68. Huber B, Feldmann F, Kothe M, Vandamme P, Wopperer J, Riedel K, Eberl L. 2004. Identification of a novel virulence factor in Burkholderia cenocepacia H111 required for efficient slow killing of Caenorhabditis elegans. Infect Immun 72:7220–7230. https://doi.org/10.1128/IAI.72.12.7220-7230.2004.

69. Aubert DF, O'Grady EP, Hamad MA, Sokol PA, Valvano MA. 2013. The Burkholderia cenocepacia sensor kinase hybrid AtsR is a global regulator modulating quorum-sensing signalling. Environ Microbiol 15:372–385. https://doi.org/10.1111/j.1462-2920.2012.02828.x.

70. O'Grady EP, Nguyen DT, Weisskopf L, Eberl L, Sokol PA. 2011. The Burkholderia cenocepacia LysR-type transcriptional regulator ShvR influences expression of quorum-sensing, protease, type II secretion, and afc genes. J Bacteriol 193:163–176. https://doi.org/10.1128/JB.00852-10.

71. Schmid N, Pessi G, Deng Y, Aguilar C, Carlier AL, Grunau A, Omasits U, Zhang LH, Ahrens CH, Eberl L. 2012. The AHL- and BDSF-dependent quorum sensing systems control specific and overlapping sets of genes in Burkholderia cenocepacia H111. PLoS One 7:e49966. https://doi.org/10.1371/journal.pone.0049966.

72. Malott RJ, Baldwin A, Mahenthiralingam E, Sokol PA. 2005. Characterization of the cciIR quorum-sensing system in Burkholderia cenocepacia. Infect Immun 73:4982–4992. https://doi.org/10.1128/IAI.73.8.4982-4992.2005.

73. O'Grady EP, Viteri DF, Sokol PA. 2012. A unique regulator contributes to quorum sensing and virulence in Burkholderia cenocepacia. PLoS One 7:e37611. https://doi.org/10.1371/journal.pone.0037611.

74. Hoffman EA, Frey BL, Smith LM, Auble DT. 2015. Formaldehyde crosslinking: a tool for the study of chromatin complexes. J Biol Chem 290:26404–26411. https://doi.org/10.1074/jbc.R115.651679.

75. Larsen JC, Szymanski C, Guerry P. 2004. N-linked protein glycosylation is required for full competence in Campylobacter jejuni 81–176. J Bacteriol 186:6508–6514. https://doi.org/10.1128/JB.186.19.6508-6514.2004.

76. Parker BL, Burchfield JG, Clayton D, Geddes TA, Payne RJ, Kiens B, Wojtaszewski JFP, Richter EA, James DE. 2017. Multiplexed temporal quantification of the exercise-regulated plasma peptidome. Mol Cell Proteomics 16:2055–2068. https://doi.org/10.1074/mcp.RA117.000020.

77. Nothaft H, Szymanski CM. 2019. New discoveries in bacterial N-glycosylation to expand the synthetic biology toolbox. Curr Opin Chem Biol 53:16–24. https://doi.org/10.1016/j.cbpa.2019.05.032.

78. Young NM, Brisson JR, Kelly J, Watson DC, Tessier L, Lanthier PH, Jarrell HC, Cadotte N, St Michael F, Aberg E, Szymanski CM. 2002. Structure of the N-linked glycan present on multiple glycoproteins in the Gram-negative bacterium, Campylobacter jejuni. J Biol Chem 277:42530–42539. https://doi.org/10.1074/jbc.M206114200.

79. Wacker M, Linton D, Hitchen PG, Nita-Lazar M, Haslam SM, North SJ, Panico M, Morris HR, Dell A, Wren BW, Aebi M. 2002. N-linked glycosylation in Campylobacter jejuni and its functional transfer into E. coli. Science 298:1790–1793. https://doi.org/10.1126/science.298.5599.1790.

80. Wong YC, Abd El Ghany M, Ghazzali RNM, Yap SJ, Hoh CC, Pain A, Nathan S. 2018. Genetic determinants associated with in vivo survival of Burkholderia cenocepacia in the Caenorhabditis elegans model. Front Microbiol 9:1118. https://doi.org/10.3389/fmicb.2018.01118.

81. Sambrook J, Fritsch EF, Maniatis T. 1989. Molecular cloning: a laboratory manual, 2nd ed. Cold Spring Harbor Laboratory, Cold Spring Harbor, NY.

82. Gibson DG, Young L, Chuang RY, Venter JC, Hutchison CA, III, Smith HO. 2009. Enzymatic assembly of DNA molecules up to several hundred kilobases. Nat Methods 6:343–345. https://doi.org/10.1038/nmeth.1318.

83. Flannagan RS, Linn T, Valvano MA. 2008. A system for the construction of targeted unmarked gene deletions in the genus Burkholderia. Environ Microbiol 10:1652–1660. https://doi.org/10.1111/j.1462-2920.2008.01576.x.

84. Aubert DF, Hamad MA, Valvano MA. 2014. A markerless deletion method for genetic manipulation of Burkholderia cenocepacia and other multidrug-resistant Gram-negative bacteria. Methods Mol Biol 1197:311–327. https://doi.org/10.1007/978-1-4939-1261-2_18.

85. Qin H, Wang Y. 2009. Exploring DNA-binding proteins with in vivo chemical cross-linking and mass spectrometry. J Proteome Res 8:1983–1991.

86. Scott NE, Parker BL, Connolly AM, Paulech J, Edwards AV, Crossett B, Falconer L, Kolarich D, Djordjevic SP, Hojrup P, Packer NH, Larsen MR, Cordwell SJ. 2011. Simultaneous glycan-peptide characterization using hydrophilic interaction chromatography and parallel fragmentation by CID, higher energy collisional dissociation, and electron transfer dissociation MS applied to the N-linked glycoproteome of Campylobacter jejuni. Mol Cell Proteomics 10:M000031. https://doi.org/10.1074/mcp.M000031-MCP201.

87. Ishihama Y, Rappsilber J, Mann M. 2006. Modular stop and go extraction tips with stacked disks for parallel and multidimensional peptide fractionation in proteomics. J Proteome Res 5:988–994. https://doi.org/10.1021/pr050385q.

88. Rappsilber J, Mann M, Ishihama Y. 2007. Protocol for micro-purification, enrichment, pre-fractionation and storage of peptides for proteomics using StageTips. Nat Protoc 2:1896–1906. https://doi.org/10.1038/nprot.2007.261.

89. Cox J, Mann M. 2008. MaxQuant enables high peptide identification rates, individualized p.p.b.-range mass accuracies and proteome-wide protein quantification. Nat Biotechnol 26:1367–1372. https://doi.org/10.1038/nbt.1511.

90. Varga JJ, Losada L, Zelazny AM, Kim M, McCorrison J, Brinkac L, Sampaio EP, Greenberg DE, Singh I, Heiner C, Ashby M, Nierman WC, Holland SM, Goldberg JB. 2013. Draft genome sequences of Burkholderia cenocepacia ET12 lineage strains K56-2 and BC7. Genome Announc 1:e00841-13. https://doi.org/10.1128/genomeA.00841-13.

91. Vizcaino JA, Csordas A, del-Toro N, Dianes JA, Griss J, Lavidas I, Mayer G, Perez-Riverol Y, Reisinger F, Ternent T, Xu QW, Wang R, Hermjakob H. 2016. 2016 update of the PRIDE database and its related tools. Nucleic Acids Res 44:D447–D456. https://doi.org/10.1093/nar/gkv1145.

92. Duan K, Dammel C, Stein J, Rabin H, Surette MG. 2003. Modulation of Pseudomonas aeruginosa gene expression by host microflora through interspecies communication. Mol Microbiol 50:1477–1491. https://doi.org/10.1046/j.1365-2958.2003.03803.x.

93. Le Guillouzer S, Groleau M-C, Déziel E. 2017. The complex quorum sensing circuitry of Burkholderia thailandensis is both hierarchically and homeostatically organized. mBio 8:e01861-17. https://doi.org/10.1128/mBio.01861-17.

94. Peeters E, Nelis HJ, Coenye T. 2008. Resistance of planktonic and biofilm-grown Burkholderia cepacia complex isolates to the transition metal gallium. J Antimicrob Chemother 61:1062–1065. https://doi.org/10.1093/jac/dkn072.

95. Tomlin KL, Malott RJ, Ramage G, Storey DG, Sokol PA, Ceri H. 2005. Quorum-sensing mutations affect attachment and stability of Burkholderia cenocepacia biofilms. Appl Environ Microbiol 71:5208–5218. https://doi.org/10.1128/AEM.71.9.5208-5218.2005.

96. O'Toole GA. 2011. Microtiter dish biofilm formation assay. J Vis Exp https://doi.org/10.3791/2437.

97. Seed KD, Dennis JJ. 2008. Development of Galleria mellonella as an alternative infection model for the Burkholderia cepacia complex. Infect Immun 76:1267–1275. https://doi.org/10.1128/IAI.01249-07.

98. Schwyn B, Neilands JB. 1987. Universal chemical assay for the detection and determination of siderophores. Anal Biochem 160:47–56. https://doi.org/10.1016/0003-2697(87)90612-9.

99. Louden BC, Haarmann D, Lynne AM. 2011. Use of blue agar CAS assay for siderophore detection. J Microbiol Biol Educ 12:51–53. https://doi.org/10.1128/jmbe.v12i1.249.

100. Edgington-Mitchell LE, Barlow N, Aurelio L, Samha A, Szabo M, Graham B, Bunnett N. 2017. Fluorescent diphenylphosphonate-based probes for detection of serine protease activity during inflammation. Bioorg Med Chem Lett 27:254–260. https://doi.org/10.1016/j.bmcl.2016.11.064.

101. Kasperkiewicz P, Altman Y, D'Angelo M, Salvesen GS, Drag M. 2017. Toolbox of fluorescent probes for parallel imaging reveals uneven location of serine proteases in neutrophils. J Am Chem Soc 139:10115–10125. https://doi.org/10.1021/jacs.7b04394.

102. Kasperkiewicz P, Poreba M, Snipas SJ, Parker H, Winterbourn CC, Salvesen GS, Drag M. 2014. Design of ultrasensitive probes for human neutrophil elastase through hybrid combinatorial substrate library pro-

filing. Proc Natl Acad Sci U S A 111:2518–2523. https://doi.org/10.1073/pnas.1318548111.

103. Liu Y, Patricelli MP, Cravatt BF. 1999. Activity-based protein profiling: the serine hydrolases. Proc Natl Acad Sci U S A 96:14694–14699. https://doi.org/10.1073/pnas.96.26.14694.

104. Darling P, Chan M, Cox AD, Sokol PA. 1998. Siderophore production by cystic fibrosis isolates of Burkholderia cepacia. Infect Immun 66:874–877.

105. Figurski DH, Helinski DR. 1979. Replication of an origin-containing derivative of plasmid RK2 dependent on a plasmid function provided in trans. Proc Natl Acad Sci USA 76:1648–1652. https://doi.org/10.1073/pnas.76.4.1648.

106. Hamad MA, Di Lorenzo F, Molinaro A, Valvano MA. 2012. Aminoarabinose is essential for lipopolysaccharide export and intrinsic antimicrobial peptide resistance in Burkholderia cepacia. Mol Microbiol 85:962–974. https://doi.org/10.1111/j.1365-2958.2012.08154.x.